

Current Biology

Parrot Genomes and the Evolution of Heightened Longevity and Cognition

Highlights

- The blue-fronted Amazon, *Amazona aestiva*, and other parrots share unique novel genes
- Convergent selection in long-lived birds suggests new lifespan-influencing genes
- Parrot genomes share genetic changes related to genes critical for brain function
- Similar changes in parrot and human genomes suggest convergent evolution of cognition

Authors

Morgan Wirthlin, Nicholas C.B. Lima, Rafael Lucas Muniz Guedes, ..., Ana Tereza R. Vasconcelos, Francisco Prosdocimi, Claudio V. Mello

Correspondence

prosdocimi@bioqmed.ufrj.br (F.P.), melloc@ohsu.edu (C.V.M.)

In Brief

The genetic basis for the complex traits that characterize parrots, including extreme longevity and advanced cognition, remains unknown. Wirthlin et al. present the genome of the blue-fronted Amazon, *Amazona aestiva*. Comparisons with other birds and humans reveal genomic similarities, suggesting convergent mechanisms in the evolution of these traits.



Parrot Genomes and the Evolution of Heightened Longevity and Cognition

Morgan Wirthlin,^{1,14,16} Nicholas C.B. Lima,^{2,15,16} Rafael Lucas Muniz Guedes,³ André E.R. Soares,³ Luiz Gonzaga P. Almeida,³ Nathalia P. Cavaleiro,³ Guilherme Loss de Moraes,³ Anderson V. Chaves,⁴ Jason T. Howard,^{5,6} Marcus de Melo Teixeira,⁷ Patricia N. Schneider,⁸ Fabrício R. Santos,⁹ Michael C. Schatz,¹⁰ Maria Sueli Felipe,¹¹ Cristina Y. Miyaki,¹² Alexandre Aleixo,¹³ Maria P.C. Schneider,⁸ Erich D. Jarvis,^{5,6} Ana Tereza R. Vasconcelos,³ Francisco Prosdocimi,^{2,*} and Claudio V. Mello^{1,17,*}

¹Department of Behavioral Neuroscience, Oregon Health & Science University, Portland, OR 97239, USA

²Laboratório de Genômica e Biodiversidade, Instituto de Bioquímica Médica Leopoldo de Meis, Universidade Federal do Rio de Janeiro, Rio de Janeiro, RJ 21941-902, Brazil

³Laboratório Nacional de Computação Científica, Rua Getúlio Vargas 333, Quitandinha, Petrópolis, RJ 25651-070, Brazil

⁴Programa de Pós-graduação em Manejo e Conservação de Ecossistemas Naturais e Agrários, Instituto de Ciências Biológicas e da Saúde, Universidade Federal de Viçosa, Florestal, Minas Gerais, Brazil

⁵Laboratory of Neurogenetics of Language, Rockefeller University, New York, NY 10065, USA

⁶Howard Hughes Medical Institute, Chevy Chase, MD 20815, USA

⁷Núcleo de Medicina Tropical, Faculdade de Medicina, Universidade de Brasília, Brasília, DF 70910-900, Brazil

⁸Instituto de Ciências Biológicas, Universidade Federal do Pará, Belém, PA, Brazil

⁹Departamento de Genética, Ecologia e Evolução, Instituto de Ciências Biológicas, Universidade Federal de Minas Gerais, Belo Horizonte, MG, Brazil

¹⁰Departments of Computer Science and Biology, Johns Hopkins University, Baltimore, MD 21218, USA

¹¹Programa de Ciências Genômicas e Biotecnologia, Universidade Católica de Brasília e Depto. de Biologia Celular, Universidade de Brasília, Brasília, DF, Brazil

¹²Instituto de Biociências, Universidade de São Paulo, R. do Matão, 277, São Paulo, SP 05508-090, Brazil

¹³Coordenação de Zoologia, Museu Paraense Emílio Goeldi, Belém, PA 66040-170, Brazil

¹⁴Present address: Computational Biology Department, Carnegie Mellon University, Pittsburgh, PA 15213, USA

¹⁵Present address: Departamento de Bioquímica e Biologia Molecular, Universidade Federal do Ceará, Fortaleza, CE 60020-181, Brazil

¹⁶These authors contributed equally

¹⁷Lead Contact

*Correspondence: prosdocimi@bioqmed.ufrj.br (F.P.), melloc@ohsu.edu (C.V.M.)

<https://doi.org/10.1016/j.cub.2018.10.050>

SUMMARY

Parrots are one of the most distinct and intriguing groups of birds, with highly expanded brains [1], highly developed cognitive [2] and vocal communication [3] skills, and a long lifespan compared to other similar-sized birds [4]. Yet the genetic basis of these traits remains largely unidentified. To address this question, we have generated a high-coverage, annotated assembly of the genome of the blue-fronted Amazon (*Amazona aestiva*) and carried out extensive comparative analyses with 30 other avian species, including 4 additional parrots. We identified several genomic features unique to parrots, including parrot-specific novel genes and parrot-specific modifications to coding and regulatory sequences of existing genes. We also discovered genomic features under strong selection in parrots and other long-lived birds, including genes previously associated with lifespan determination as well as several hundred new candidate genes. These genes support a range of cellular functions, including telomerase activity; DNA damage repair; control of cell proliferation, cancer, and immunity; and anti-oxidative mechanisms.

We also identified brain-expressed, parrot-specific paralogs with known functions in neural development or vocal-learning brain circuits. Intriguingly, parrot-specific changes in conserved regulatory sequences were overwhelmingly associated with genes that are linked to cognitive abilities and have undergone similar selection in the human lineage, suggesting convergent evolution. These findings bring novel insights into the genetics and evolution of longevity and cognition, as well as provide novel targets for exploring the mechanistic basis of these traits.

RESULTS AND DISCUSSION

Parrots (order Psittaciformes) possess several attributes that make them excellent models for understanding the evolution of complex traits. Like humans, parrots as a group have (1) large brains relative to body size [1], (2) a high density of neurons in the forebrain [5], (3) advanced cognitive abilities including object permanence and tool use [6], (4) complex social organization [7], (5) vocalizations learned through cultural transmission using specialized brain circuits [3], (6) cooperative problem solving [8], (7) extended developmental and rearing periods [9], and (8) exceptional longevity, especially given their high metabolism



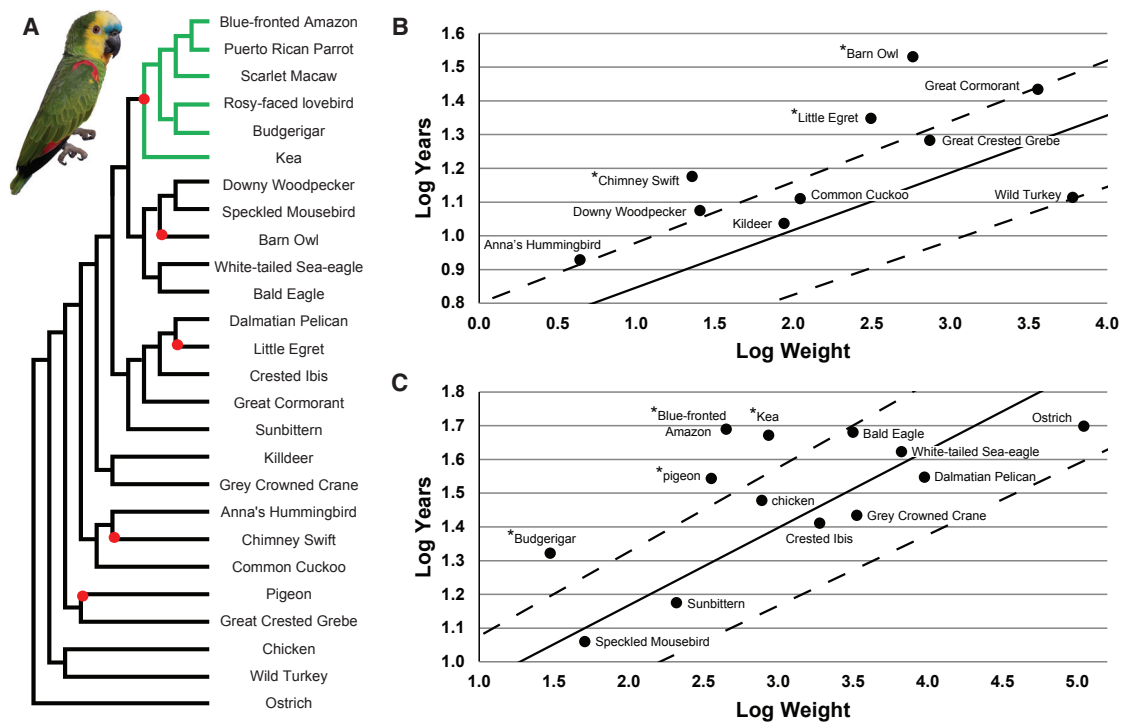


Figure 1. Phylogenetic Relationships and Longevity of Parrots, Including *Amazona aestiva*, in Relation to Other Birds

(A) This schematic phylogeny, derived from previously published studies [10, 11], depicts the relationship between parrots and all other birds analyzed in the longevity analyses. Red nodes indicate the occurrence of high longevity and were used as branches to test for nonneutral sequence evolution in long-lived birds against a null model using a likelihood ratio test. The photo depicts Moises, the adult male blue-fronted Amazon whose genome was sequenced for this study. (B and C) The expected lifespan of the 23 bird species analyzed for genomic signatures of longevity in plotted as a solid line, based on calculations derived from Prinzing [12] that describe the relationship between mass (log weight) and longevity (log years) for wild (B) and captive (C) birds (see STAR Methods: Longevity). Species falling outside of the dashed lines deviate significantly from expected lifespan based on mass and are indicated with an “*.” See also Table S1.

[4]. The genetic basis for characteristic parrot traits remains unknown, and no attempt has yet been made to identify genomic features unique to parrots. Genome assemblies are available for the Puerto Rican parrot, scarlet macaw, rosy-faced lovebird, budgerigar, and kea, representing a broad sampling of extant parrot diversity [10] (Figure 1). However, with the exception of the budgerigar's, these genomes have been described in low coverage and/or low contiguity (STAR Methods: Genome Sequencing).

To address these questions, we generated a high-coverage (120.6×) genome assembly for the blue-fronted Amazon (*Amazona aestiva*, Linnaeus, 1758). Emblematic of the Brazilian avifauna, this highly vocal parrot species is exceptionally long lived, even among parrots, with confirmed cases of birds living up to 66 years in captivity and anecdotal reports of at least 90 years [13]. The resultant assembly (Aaes1) contains 3,232 scaffolds with a scaffold N50 size of 1.09 Mb and a contig N50 size of 27.8 kb, surpassing all previous parrot genome assemblies in sequence contiguity (STAR Methods: Genome Sequencing). Genome annotation revealed the *A. aestiva* genome to be comparable to other avian genomes in terms of coding genes, miRNAs, and repetitive content [11]. We also provide a set of 3,516 microsatellites with primers that will benefit future conservation, population genetics, and phylogeographic efforts (STAR Methods: Annotation).

A genome-wide comparison of *A. aestiva* and 4 other parrots with multiple non-parrot outgroups identified a substantial amount of genomic material unique to parrots (STAR Methods: Genome Sequencing). This included a set of novel, parrot-specific genes, resulting from paralogous gene duplications, gene family expansions from successive rounds of duplication, or *de novo* genes with no known paralog in other species (Table 1; STAR Methods: Novel Genes). There were also numerous non-coding scaffolds likely representing intergenic regions. In limited cases, the mechanism of duplication could be attributed to chromosomal rearrangements (Figure S1). This finding is consistent with our previous findings of gene duplication at chromosomal breakpoints in birds [14].

Insights into Longevity from Parrots and Other Long-Lived Birds

To gain insight into the genetic underpinnings of longevity, we analyzed 23 bird species with reliable longevity data and available genome assemblies for genomic signatures of selection in long-lived birds. We divided species into high-longevity (HL; maximum recorded longevity at least 20% higher than predicted by body mass [12, 15]) and regular-longevity (RL; maximum recorded longevity corresponding to or lower than that predicted by body mass) groups (Figure 1A; Table S1), using estimated corrections for wild versus captive birds (Figures 1B and 1C;

Table 1. Novel Genes in Parrot Genomes

Parent Gene	Gene Function Summary	Budgerigar Brain Expression
Novel Genes Conserved in Parrots (Single Duplication Event)		
ARPC4-TTLL3L	cytoskeletal structural integrity	no
CEP83	structural integrity of cilia	yes
DESI2 ^{a,b}	post-translational modification	yes
PLXNC1	axon guidance	yes
PRKAR2A	cyclic AMP-dependent signaling	yes
PSMD6 ^{a,b}	protease	yes
RSPH3	cyclic AMP-dependent signaling	no
SIDT1	intercellular RNA transfer	no
SLC9A5	Na-H exchanger	no
TAGAP	T cell Rho-gap signaling	no
TAX1BP3	signal transduction	yes
ZNF541 ^a	transcription factor	no
Gene Families Expanded in Parrots (Multiple Duplication Events)		
AMY1	dietary starch digestion	–
GPI-anchored protein 58	unknown	–
LRR37A	innate immunity	–
MROH7	unknown	–
MXRA7	matrix remodeling	–
TAGAP	T cell Rho-gap signaling	–
TTLL3	cytoskeletal structural integrity	–
SUN2	DNA repair	–

Summary of novel genes found uniquely in parrot genomes. We identify 12 genes that have undergone duplication since the split from the last common ancestor of parrots and songbirds but before the diversification of the extant parrot clade. In 6 out of 12 (50%), we detect evidence of expression in the budgerigar brain. We also identify 8 expanded gene families that have undergone multiple rounds of gene duplication in parrots. We also identify a set of putative *de novo* novel genes found uniquely in parrots with no apparent orthologs in any other bird groups. Supporting their validity, 79 out of 136 *de novo* novel gene predictions (58%) contain predicted protein domains, and for 17 (12.5%) we detect evidence of expression in the budgerigar brain. Additional details and full list of novel genes are presented in [STAR Methods: Novel Genes](#).

^aAvian ortholog cannot be unambiguously identified.

^bGene duplication in conjunction with chromosomal breakpoint event (see [Figure S1](#)).

STAR Methods: Longevity. Besides parrots, HL birds included several other notably long-lived species (rock dove, chimney swift, little egret, and barn owl). Importantly, high longevity is most parsimoniously interpreted as having evolved independently in these avian groups, as is clearly seen when examining the distribution of this trait mapped onto the currently accepted avian phylogeny ([Figure 1A](#)).

We initially searched for the largest possible set of orthologs unequivocally present in all 23 species with high-quality longevity data, resulting in 4,132 single gene ortholog clusters (SGOs; gene sets containing one copy from all birds analyzed). We utilized a phylogeny-based likelihood-ratio test to test for significant group differences in the ratio of nonsynonymous-to-synonymous nucleotide substitutions (dn/ds, or ω) indicative of

evolutionary selective pressure [16]. We obtained evidence of differential rates of evolution between HL and RL birds in 344 genes (8%) ([Figure 2A](#); [STAR Methods: Longevity](#)). Of these, 281 genes had greater ω in the HL group, indicative of more relaxed sequence constraint (favoring variation leading to new functions), whereas the remaining 63 had lower ω in HL birds, suggesting higher stabilizing selection in these genes. Separately, we also detected evidence of positive selection at 90 amino acid sites in 31 proteins, 39 of these within known functional domains ([Data S1](#)).

A subset ($n = 20$; 6%) of the 344 genes under selection in HL birds have been experimentally shown to impact lifespan in other model organisms (GenAge [15]) ([Figure 2A](#)). Besides validating our analyses, this observation supports an association of these genes with lifespan determination in birds as well. The remaining genes ($n = 324$, or 94%) had never previously been associated with lifespan determination in any organism to our knowledge, representing promising novel candidates for involvement in longevity ([STAR Methods: Longevity](#)). Functional annotation clustering of all genes under selection in long-lived birds revealed highly significant enrichments in annotations related to cell division, cell-cycle regulation, and RNA splicing and processing, as well as weaker but significant enrichments in DNA damage and repair, mitochondrial function, and oxidative metabolism ([Figure 2B](#); [Table S2](#)).

Within the GenAge subset, the strongest evidence of selective pressure was for *TERT* (telomerase reverse transcriptase), a key component of the telomerase complex that confers protection against cell senescence [15]. *TERT* also showed two positively selected sites ([Figure 2C](#); [Data S1](#)) within the reverse transcriptase domain in long-lived birds, in proximity to sites critical for catalytic function ([Figure 2D](#)). These observations suggest that changes in the *TERT* catalytic activity may represent a fundamental longevity-promoting mechanism and substantiate findings that telomerase activity is altered in long-lived birds [17]. Among the genes not previously reported in GenAge, a large subset showed involvement in DNA damage and repair, including *POLK*, which allows for the DNA replication machinery to bypass sites of DNA lesion, and *ERCC3*, a helicase that repairs nucleotide excisions ([Figure 2B](#)).

While protective against cell senescence, high *TERT* activity comes with risks of an increased rate of uncontrolled proliferation and tumor formation [18]. Highlighting the importance of balancing these processes, we found that several genes under selective pressure in long-lived birds (*BUB1B*, *BUB3*, *KIF4A*, *KIF1BP*, and *CCNE1*) have been linked to the control of cell proliferation and tumor proliferation. Specific mechanisms include regulation of the spindle assembly during cell division by mitotic checkpoint proteins, control of chromosome integrity during mitosis by microtubule-based motor protein, and control of cell-cycling and tumor-suppression mechanisms ([Figure 2B](#); [Table S2](#)). Based on these findings, we suggest that the balanced coevolution of pathways for telomerase activity and cell-cycle regulation may represent a mechanism for preventing increased rates of cancer in the evolution of increased longevity in birds.

Further highlighting DNA repair and control of cell proliferation as important pathways in the evolution of parrots, several duplicated genes in parrots also regulate genomic stability and cell senescence. These include *PSMD6*, which encodes a 26S

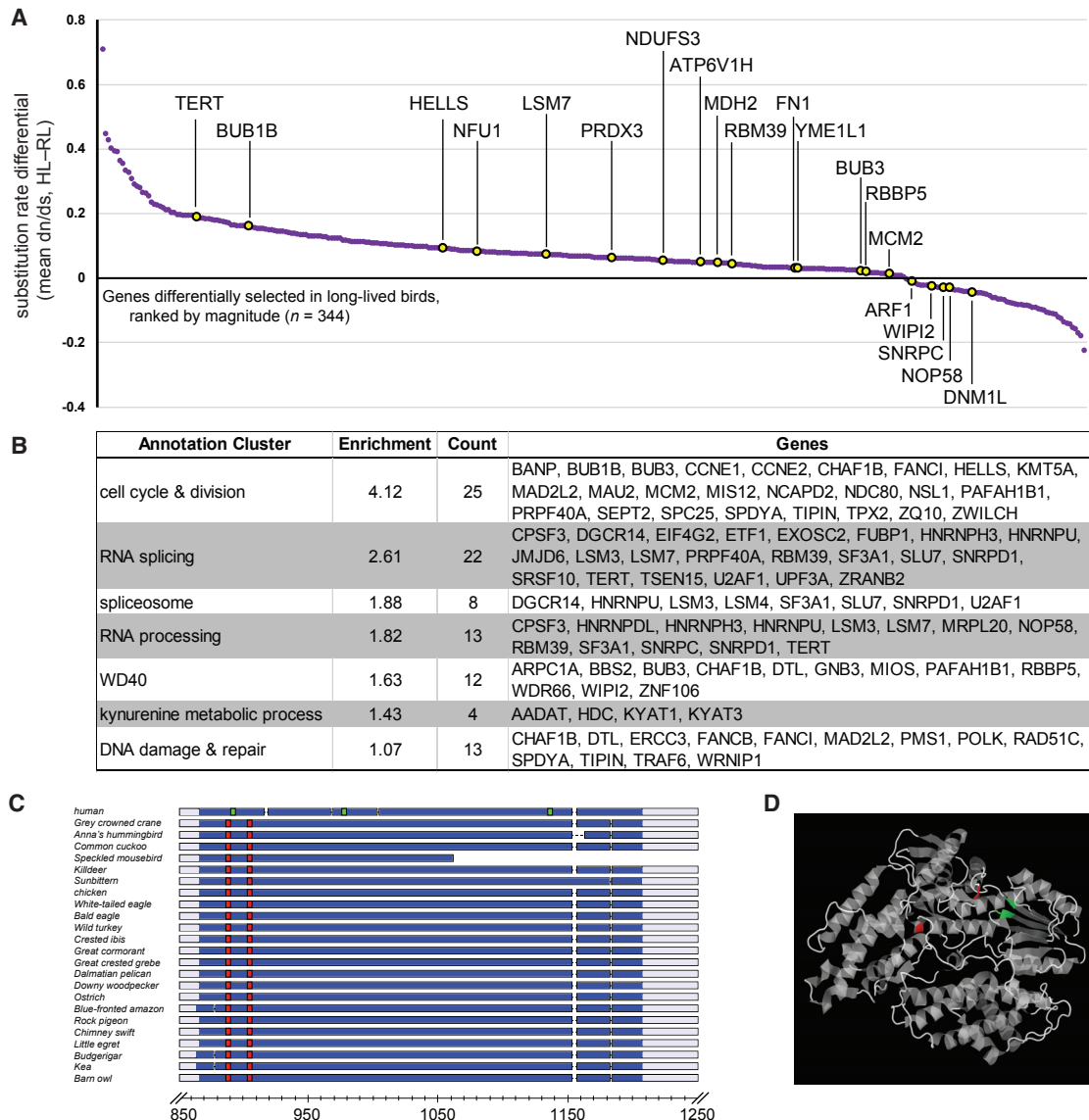


Figure 2. Genes Under Positive Selection in Long-Lived Birds

(A) Plot of the strength of selective pressure for the set of genes with significantly different nonsynonymous to synonymous substitution ratios (dn/ds, or ω) between high-longevity (HL) birds and regular-longevity (RL) birds (baseline). Genes with known lifespan effect in model systems (from GenAge [15]) are highlighted in yellow; candidate longevity-influencing genes with no previously reported lifespan data are highlighted in purple.

(B) Table of the major gene functional categories enriched in genes with differential selection in HL birds.

(C) Comparative multiple sequence alignment of *TERT* proteins across avian species and humans, with sites under positive selection in long-lived birds indicated in red and metal binding sites in green, all occurring within the reverse transcriptase domain, in blue. Scales indicate amino acid position within alignments.

(D) Crystal structure of *TERT* reverse transcriptase catalytic subunit. Positively selected residues are in red, which are in close physical proximity to metal binding sites critical for catalytic activity, in green. PDB: *TERT*, 3DU6.

See also Table S2 and Data S1.

proteasome subunit that colocalizes with DNA damage foci in cells that have suffered genotoxic damage, helping to ensure that these cells are targeted for senescence, and *DES12*, an apoptosis regulator and part of the early response to DNA damage (see Figures S1A and S1B for a depiction of gene duplication and supportive evidence of gene function).

Parrots and other HL birds also exhibited selection in *SOD1* and *SOD3*, genes essential for protection from oxidative damage

stress [19]. We found that *SOD3* exhibits high stabilizing selection in HL birds relative to RL birds (STAR Methods: Longevity). Several positively selected sites in *SOD1* were within the predicted Cu-Zn binding domain (Data S1), likely modulating metal binding affinity and enzymatic activity [19]. The “free radical hypothesis of aging,” which postulates that increased longevity in birds depends on protection against oxidative damage by free radicals, has been challenged by a failure to detect tissue

differences in indicators of oxidative stress when comparing similar sized long- versus short-lived birds [20]. Our finding of convergent selection in these genes, as well as in several others involved in oxidative stress and/or mitochondrial functions in independent avian lineages, supports the importance of anti-oxidative protection in the evolution of avian longevity [21]. Further investigation of the specific role of superoxide dismutase in long-lived birds could serve to reconcile the contrasting findings in the previous literature. Lastly, we note a large and significant gene subset related to RNA splicing and processing (Figure 2B; Table S2), which for the most part was not previously reported in GenAge, although a causal relation to lifespan determination is unclear.

Overall, our findings suggest that changes in telomerase, DNA repair, cell-cycle progression, RNA splicing and processing, and oxidative stress pathways may be critical for heightened longevity in birds. They also provide candidate genes and amino acid sites for future experimental interrogation that could lead to advances in our understanding of lifespan extension. Although genomic studies of individual species with high longevity have been performed previously [16, 22], this study represents, to our knowledge, the largest comparative genomic analysis of long-lived vertebrates to date. Because these genes have independently experienced high rates of sequence substitution across multiple long-lived lineages, they could reflect fundamental mechanisms associated with the evolution of heightened longevity.

Insights into Cognition from Parrot Genomes

Supporting our initial hypothesis that novel genes in parrots might relate to brain function and cognition, the ancestral parent gene paralogs of several parrot novel genes have known involvement in neuronal development, physiology, and behavior (Table 1). Most prominently, *PLXNC1* was uniquely duplicated in parrots among the bird species examined (Figure S1C). *PLXNC1*, a regulator of axonal outgrowth, is one of a distinct set of genes with shared differential expression in the specialized vocal-learning motor-cortical areas of humans, parrots, hummingbirds, and songbirds [23]. This convergent molecular specialization in unrelated vocal learning groups is consistent with the hypothesis that regulation of cortical projections within vocal-motor circuits may be critical to the evolution of vocal learning systems [23]. Determining redundant versus complementary or modulatory roles for the duplicate *PLXNC1*s represents an important target for gene manipulation studies.

The parent paralogs of several other parrot-specific duplicated genes (*CEP83*, *SLC9A5*, *RSPH3*, and *LRR37A*; Table 1) are involved in critical aspects of neuronal cell structure and integrity, including regulation of actin cytoskeleton, microtubule sliding, filopodial extension, and the structure of cilia and dendritic spines, disruptions of which can lead to cognitive impairment [24–27]. *LRR37A*, in particular, is a member of a large gene family with involvement in the immune system and in nervous system development, and which is greatly expanded in primates [26]. In humans, *LRR37* is broadly expressed, with enrichment in the cerebellum and thymus [26]. Our evidence of a duplication in parrots points to a convergent expansion of this gene family in both primates and parrots, suggesting a possible link with the increased cognitive capacities of these two unrelated taxa.

We further identified a set of parrot *de novo* novel genes (present in parrot genomes with no paralogs in other species) with evidence of brain expression ($n = 1$; Table 1; STAR Methods: Novel Genes). Although all contain open reading frames, roughly half ($n = 9$; 53%) contain no known functional domains. Whether these expressed transcripts are actually translated or represent regulatory non-coding RNAs and whether they have been integrated into functional pathways or represent non-functional “proto-genes” [28] are questions that will require further analysis. However, given the precedent in songbirds, where some *de novo* genes have been shown to be specifically expressed in brain structures devoted to vocal learning behavior [14], parrot *de novo* genes represent promising candidates for regulating brain regions involved in vocal learning, cognition, and other parrot lineage traits.

Noncoding genomic regions can contribute to trait evolution through changes in gene regulatory elements that cannot be detected by analysis of coding sequences only. To determine whether parrots possess lineage-specific variation in *cis*-regulatory sequences that could contribute to brain function and cognition, we investigated ultra-conserved noncoding elements (UCNEs; noncoding sequences highly conserved throughout vertebrate phylogeny), which are often associated with enhancers that play critical, conserved roles in development [29]. We found a suite of UCNEs with significant sequence divergence in parrot genomes relative to other vertebrates (Table 2; STAR Methods: UCNEs). Remarkably, of the 11 protein-coding genes associated with parrot-divergent UCNEs, 10 (91%) are involved in various aspects of brain function, including forebrain patterning, neuronal subtype differentiation, and adult neurogenesis [30–38] (Table 2). Supporting their activity in the brain, we found budgerigar brain transcriptomic evidence of expression for 9 of these genes (Table 2). The majority of these ($n = 7$) showed similar evolutionary selection in the human lineage, as evidenced by association with conserved noncoding elements divergent in humans relative to great apes and other mammals [39, 40] (Table 2, Figure S2).

Among the 11 genes with regulatory regions containing parrot-divergent UCNEs, a subset is associated with diseases that disrupt cognitive function in humans (Table 2). Noteworthy is *AUTS2*, whose mutations in humans are associated with a range of cognitive disabilities including autism, intellectual impairment, developmental delay, and language deficits [30]. *AUTS2* has also received attention as a gene that may have been critical to the evolution of human cognitive abilities [30]. Also noteworthy are *NPAS3*, in which breakpoint translocations result in schizophrenia and intellectual disability [35], and *BCL11A*, a regulator of axonal branching and outgrowth in developing neurons, in which deletions result in brain malformation and intellectual disability [31]. Two further genes, *ERBB4* and *ESRRG*, have known associations with cognitive disorders, with variants established as risk factors for schizophrenia [33, 34]. These results suggest that humans and parrots may have undergone convergent selection in the regulatory regions of a crucial set of genes related to brain development and cognition.

Conclusions

Parrot genomes are distinguished by the presence of domain-specific modifications in existing gene cohorts, novel genes,

Table 2. Genes Associated with Ultra-Conserved Noncoding Elements Divergent in Parrots

Gene	haCNSs Associated with Gene	HARs Associated with Gene	Associations with Brain Function and Cognitive Disorders	Brain Expressed in Budgerigar
AUTS2	HACNS174, HACNS369	HAR31	forebrain development, autism related [30]	yes
BCL11A	HACNS101	HAR180	neuron projection development, intellectual disability related [31]	yes
EBF3	–	–	cortical development, intellectual disability related [32]	no
ERBB4	HACNS183, HACNS505, HACNS977	HAR84	forebrain patterning, schizophrenia related [33]	yes
ESRRG	–	HAR177	schizophrenia related [34]	yes
NPAS3	HACNS96, HACNS221, HACNS490, HACNS553, HACNS658	HAR21, HAR89, HAR96, HAR173, HAR189, HAR202	adult neurogenesis, schizophrenia and intellectual disability related [35]	yes
PROX1	HACNS878	–	forebrain neuron differentiation, adult neurogenesis [36]	yes
SOX6	–	–	neuronal differentiation [37]	yes
SP8	–	–	forebrain patterning [38]	yes
ZC3H3	HACNS71	–	no known brain function	yes
ZNF608	HACNS214, HACNS852	–	no known brain function	yes

Genes associated with ultra-conserved noncoding elements (UCNEs) showing accelerated evolution in the blue-fronted Amazon, budgerigar, and Kea genomes. The majority of these genes are also associated with human accelerated conserved noncoding sequences (haCNSs [39]) and/or human accelerated regions (HARs [40]). See also Figure S2.

and variations in noncoding sequences thought to regulate expression. The discovery of a distinct gene set under evolutionary selection in long-lived birds provides independent support for genes previously associated with longevity in non-vertebrate model systems and identifies a large suite of genes with no previous association with longevity, representing promising targets for further experimental interrogation. Parrot-lineage-specific changes in genes and regulatory regions associated with the brain represent candidate mechanisms for the evolution of the larger brains and more advanced cognitive abilities of parrots, with intriguing parallels to evolutionary mechanisms thought to have facilitated the emergence of these traits in humans. These findings support parrots, which outperform even great apes in several measurements of intelligence [2], as an excellent experimental model for uncovering the genetic basis of higher cognition. Finally, as blue-fronted Amazon populations have declined in recent decades, owing to drastic reduction in natural habitat due to urban and agricultural expansions and illegal trading, its sequenced genome should be a valuable tool in ongoing conservation efforts.

STAR★METHODS

Detailed methods are provided in the online version of this paper and include the following:

- KEY RESOURCES TABLE
- CONTACT FOR REAGENT AND RESOURCE SHARING
- EXPERIMENTAL MODEL AND SUBJECT DETAILS
- METHOD DETAILS
 - Genome Sequencing
 - Genome Annotation
 - Longevity
 - Novel Genes
 - Ultra-Conserved Noncoding Elements

- QUANTIFICATION AND STATISTICAL ANALYSIS
- DATA AND SOFTWARE AVAILABILITY

SUPPLEMENTAL INFORMATION

Supplemental Information includes three figures, five tables, and one data file and can be found with this article online at <https://doi.org/10.1016/j.cub.2018.10.050>.

ACKNOWLEDGMENTS

This work was supported through the Brazilian Avian Genome Consortium (SIS-BIO-Aves project, coordinated by M.P.C.S., E.D.J., A.T.R.V., and C.V.M.), funded by Conselho Nacional de Desenvolvimento Científico e Tecnológico/Fundação Amazonia de Amparo a Estudos e Pesquisas (CNPq/FAPESPA; Brazil). Further funding support that contributed to this project was provided by Fundação de Amparo a Pesquisa do Estado do Rio de Janeiro (FAPERJ; Brazil) to F.P. (E-26/202.810/2015) and Howard Hughes Medical Institute (HHMI; US) to E.D.J. We also acknowledge that the comparative methods for novel genes analysis were developed with support from the NIH/National Institute of Deafness and Communication Disorders (grant R21 DC014432) to C.V.M. We would like to thank biologist Paulo Augusto Ribeiro Machado for providing access to the *A. aestiva* specimen (FVVF132).

AUTHOR CONTRIBUTIONS

C.V.M., F.P., A.T.R.V., M.d.M.T., M.S.F., M.P.C.S., and A.A. conceived the project. C.V.M. and M.P.C.S. were co-coordinators of the consortium (SISBIO-AVES) that provided funding and resources for the project. A.T.R.V., F.R.S., C.Y.M., E.D.J., M.S.F., and A.A. were participating members of the consortium. A.V.C., F.R.S., and M.d.M.T. performed sample identification, tissue collection, and DNA extraction, with contributions from A.A., P.N.S., M.S.F., and C.Y.M. J.T.H. and E.D.J. coordinated the genome sequencing. F.P., A.T.R.V., and L.G.P.A. conducted the genome assembly projects, with contributions from N.C.B.L., A.E.R.S., M.C.S., and E.D.J. N.P.C. performed the repetitive element analyses. N.C.B.L., F.P., R.L.M.G., and L.G.P.A. carried out the gene prediction and orthology annotation. M.W. and C.V.M. performed the novel gene analyses. M.W. and N.C.B.L. carried out the brain transcriptome analyses. G.L.d.M. performed the miRNA analyses. M.W., R.L.M.G., and C.V.M. performed the longevity analyses.

M.W. performed the UCNE analyses. M.W., C.V.M., F.P., and E.D.J. wrote the manuscript, with contributions from R.L.M.G., N.C.B.L., A.E.R.S., N.P.C., A.A., F.R.S., and C.Y.M. All authors read and approved the final manuscript.

DECLARATION OF INTERESTS

The authors declare no competing interests.

Received: February 11, 2016

Revised: August 14, 2018

Accepted: October 23, 2018

Published: December 6, 2018

REFERENCES

- Iwaniuk, A.N., Dean, K.M., and Nelson, J.E. (2005). Interspecific allometry of the brain and brain regions in parrots (psittaciformes): comparisons with other birds and primates. *Brain Behav. Evol.* **65**, 40–59.
- Emery, N.J. (2006). Cognitive ornithology: the evolution of avian intelligence. *Philos. Trans. R. Soc. Lond. B Biol. Sci.* **361**, 23–43.
- Brauth, S.E., Heaton, J.T., Shea, S.D., Durand, S.E., and Hall, W.S. (1997). Functional anatomy of forebrain vocal control pathways in the budgerigar (*Melopsittacus undulatus*). *Ann. N Y Acad. Sci.* **807**, 368–385.
- Munshi-South, J., and Wilkinson, G.S. (2006). Diet influences life span in parrots (Psittaciformes). *Auk* **123**, 108–118.
- Olkowicz, S., Kocourek, M., Lučan, R.K., Porteš, M., Fitch, W.T., Herculano-Houzel, S., and Némec, P. (2016). Birds have primate-like numbers of neurons in the forebrain. *Proc. Natl. Acad. Sci. USA* **113**, 7255–7260.
- Emery, N.J., and Clayton, N.S. (2005). Evolution of the avian brain and intelligence. *Curr. Biol.* **15**, R946–R950.
- Hobson, E.A., Avery, M.L., and Wright, T.F. (2014). The socioecology of monk parakeets: insights into parrot social complexity. *Auk* **131**, 756–775.
- Péron, F., Rat-Fischer, L., Lalot, M., Nagle, L., and Bovet, D. (2011). Cooperative problem solving in African grey parrots (*Psittacus erithacus*). *Anim. Cogn.* **14**, 545–553.
- Iwaniuk, A.N., and Nelson, J.E. (2003). Developmental differences are correlated with relative brain size in birds: a comparative analysis. *Can. J. Zool.* **81**, 1913–1928.
- Wright, T.F., Schirtzinger, E.E., Matsumoto, T., Eberhard, J.R., Graves, G.R., Sanchez, J.J., Capelli, S., Müller, H., Scharpegge, J., Chambers, G.K., and Fleischer, R.C. (2008). A multilocus molecular phylogeny of the parrots (Psittaciformes): support for a Gondwanan origin during the cretaceous. *Mol. Biol. Evol.* **25**, 2141–2156.
- Zhang, G., Li, C., Li, Q., Li, B., Larkin, D.M., Lee, C., Storz, J.F., Antunes, A., Greenwold, M.J., Meredith, R.W., et al.; Avian Genome Consortium (2014). Comparative genomics reveals insights into avian genome evolution and adaptation. *Science* **346**, 1311–1320.
- Prinzinger, R. (1993). Life span in birds and the ageing theory of absolute metabolic scope. *Comp. Biochem. Physiol. Part A. Physiol.* **105**, 609–615.
- Young, A.M., Hobson, E.A., Lackey, L.B., and Wright, T.F. (2012). Survival on the ark: life history trends in captive parrots. *Anim. Conserv.* **15**, 28–53.
- Wirthlin, M., Lovell, P.V., Jarvis, E.D., and Mello, C.V. (2014). Comparative genomics reveals molecular features unique to the songbird lineage. *BMC Genomics* **15**, 1082.
- Tacutu, R., Craig, T., Budovsky, A., Wuttke, D., Lehmann, G., Taranukha, D., Costa, J., Fraiefeld, V.E., and de Magalhães, J.P. (2013). Human Ageing Genomic Resources: integrated databases and tools for the biology and genetics of ageing. *Nucleic Acids Res.* **41**, D1027–D1033.
- Keane, M., Semeiks, J., Webb, A.E., Li, Y.I., Quesada, V., Craig, T., Madsen, L.B., van Dam, S., Brawand, D., Marques, P.I., et al. (2015). Insights into the evolution of longevity from the bowhead whale genome. *Cell Rep.* **10**, 112–122.
- Haussmann, M.F., Winkler, D.W., Huntington, C.E., Nisbet, I.C.T., and Vleck, C.M. (2004). Telomerase expression is differentially regulated in birds of differing life span. *Ann. N Y Acad. Sci.* **1079**, 186–190.
- Kim, N.W., Piatyszek, M.A., Prowse, K.R., Harley, C.B., West, M.D., Ho, P.L., Coviello, G.M., Wright, W.E., Weinrich, S.L., and Shay, J.W. (1994). Specific association of human telomerase activity with immortal cells and cancer. *Science* **266**, 2011–2015.
- Zelko, I.N., Mariani, T.J., and Folz, R.J. (2002). Superoxide dismutase multigene family: a comparison of the CuZn-SOD (SOD1), Mn-SOD (SOD2), and EC-SOD (SOD3) gene structures, evolution, and expression. *Free Radic. Biol. Med.* **33**, 337–349.
- Montgomery, M.K., Buttemer, W.A., and Hulbert, A.J. (2012). Does the oxidative stress theory of aging explain longevity differences in birds? II. Antioxidant systems and oxidative damage. *Exp. Gerontol.* **47**, 211–222.
- Lambert, A.J., Boysen, H.M., Buckingham, J.A., Yang, T., Podlutzky, A., Austad, S.N., Kunz, T.H., Buffenstein, R., and Brand, M.D. (2007). Low rates of hydrogen peroxide production by isolated heart mitochondria associate with long maximum lifespan in vertebrate homeotherms. *Aging Cell* **6**, 607–618.
- Keane, M., Craig, T., Alföldi, J., Berlin, A.M., Johnson, J., Seluanov, A., Gorbunova, V., Di Palma, F., Lindblad-Toh, K., Church, G.M., and de Magalhães, J.P. (2014). The Naked Mole Rat Genome Resource: facilitating analyses of cancer and longevity-related adaptations. *Bioinformatics* **30**, 3558–3560.
- Pfenning, A.R., Hara, E., Whitney, O., Rivas, M.V., Wang, R., Roulhac, P.L., Howard, J.T., Wirthlin, M., Lovell, P.V., Ganapathy, G., et al. (2014). Convergent transcriptional specializations in the brains of humans and song-learning birds. *Science* **346**, 1256846.
- Failler, M., Gee, H.Y., Joo, K., Halbritter, J., Belkacem, L., Filhol, E., Porath, J.D., Braun, D.A., Schueler, M., et al. (2014). Mutations of CEP83 cause infantile nephronophthisis and intellectual disability. *Am. J. Hum. Genet.* **94**, 905–914.
- Diering, G.H., Mills, F., Bamji, S.X., and Numata, M. (2011). Regulation of dendritic spine growth through activity-dependent recruitment of the brain-enriched Na⁺/H⁺ exchanger NHE5. *Mol. Biol. Cell* **22**, 2246–2257.
- Giannuzzi, G., Siswara, P., Malig, M., Marques-Bonet, T., Mullikin, J.C., Ventura, M., and Eichler, E.E.; NISC Comparative Sequencing Program (2013). Evolutionary dynamism of the primate LRRC37 gene family. *Genome Res.* **23**, 46–59.
- Hu, X., Yan, R., Song, L., Lu, X., Chen, S., and Zhao, S. (2014). Subcellular localization and function of mouse radial spoke protein 3 in mammalian cells and central nervous system. *J. Mol. Histol.* **45**, 723–732.
- Carvunis, A.-R., Rolland, T., Wapinski, I., Calderwood, M.A., Yildirim, M.A., Simonis, N., Charlotteaux, B., Hidalgo, C.A., Barbette, J., Santhanam, B., et al. (2012). Proto-genes and de novo gene birth. *Nature* **487**, 370–374.
- Dimitrieva, S., and Bucher, P. (2013). UCNEbase—a database of ultraconserved non-coding elements and genomic regulatory blocks. *Nucleic Acids Res.* **41**, D101–D109.
- Oksenberg, N., Stevison, L., Wall, J.D., and Ahituv, N. (2013). Function and regulation of *AUTS2*, a gene implicated in autism and human evolution. *PLoS Genet.* **9**, e1003221.
- Balci, T.B., Sawyer, S.L., Davila, J., Humphreys, P., and Dymont, D.A. (2015). Brain malformations in a patient with deletion 2p16.1: a refinement of the phenotype to BCL11A. *Eur. J. Med. Genet.* **58**, 351–354.
- Sleven, H., Welsh, S.J., Yu, J., Churchill, M.E.A., Wright, C.F., Henderson, A., Horvath, R., Rankin, J., Vogt, J., Magee, A., et al.; Deciphering Developmental Disorders study; CAUSES study (2017). De novo mutations in *EBF3* cause a neurodevelopmental syndrome. *Am. J. Hum. Genet.* **100**, 138–150.

33. Jaaro-Peled, H., Hayashi-Takagi, A., Seshadri, S., Kamiya, A., Brandon, N.J., and Sawa, A. (2009). Neurodevelopmental mechanisms of schizophrenia: understanding disturbed postnatal brain maturation through neuregulin-1-ErbB4 and DISC1. *Trends Neurosci.* *32*, 485–495.
34. Terwisscha van Scheltinga, A.F., Bakker, S.C., van Haren, N.E.M., Derks, E.M., Buizer-Voskamp, J.E., Boos, H.B.M., Cahn, W., Hulshoff Pol, H.E., Ripke, S., Ophoff, R.A., and Kahn, R.S.; Psychiatric Genome-wide Association Study Consortium (2013). Genetic schizophrenia risk variants jointly modulate total brain and white matter volume. *Biol. Psychiatry* *73*, 525–531.
35. Michaelson, J.J., Shin, M.-K., Koh, J.-Y., Bruggeman, L., Zhang, A., Katzman, A., McDaniel, L., Fang, M., Pufall, M., and Pieper, A.A. (2017). Neuronal PAS domain proteins 1 and 3 are master regulators of neuropsychiatric risk genes. *Biol. Psychiatry* *82*, 213–223.
36. Karalay, O., Doberauer, K., Vadodaria, K.C., Knobloch, M., Berti, L., Miquelajauregui, A., Schwark, M., Jagasia, R., Taketo, M.M., Tarabykin, V., et al. (2011). Prospero-related homeobox 1 gene (Prox1) is regulated by canonical Wnt signaling and has a stage-specific role in adult hippocampal neurogenesis. *Proc. Natl. Acad. Sci. USA* *108*, 5807–5812.
37. Azim, E., Jabaudon, D., Fame, R.M., and Macklis, J.D. (2009). SOX6 controls dorsal progenitor identity and interneuron diversity during neocortical development. *Nat. Neurosci.* *12*, 1238–1247.
38. Zembrzycki, A., Griesel, G., Stoykova, A., and Mansouri, A. (2007). Genetic interplay between the transcription factors Sp8 and Emx2 in the patterning of the forebrain. *Neural Dev.* *2*, 8.
39. Prabhakar, S., Noonan, J.P., Pääbo, S., and Rubin, E.M. (2006). Accelerated evolution of conserved noncoding sequences in humans. *Science* *314*, 786.
40. Pollard, K.S., Salama, S.R., King, B., Kern, A.D., Dreszer, T., Katzman, S., Siepel, A., Pedersen, J.S., Bejerano, G., Baertsch, R., et al. (2006). Forces shaping the fastest evolving regions in the human genome. *PLoS Genet.* *2*, e168.

STAR★METHODS

KEY RESOURCES TABLE

REAGENT or RESOURCE	SOURCE	IDENTIFIER
Biological Samples		
Blood: <i>Amazona aestiva</i>	This paper	Centro de Coleções Taxonômicas of Universidade Federal de Minas Gerais, Voucher #: B04212
Critical Commercial Assays		
DNeasy Blood & Tissue Kit	QIAGEN	Cat#: 69504
Nextera Mate Pair Library Preparation Kit	Illumina	Cat#: FC-132-1001
Deposited Data		
Whole genome sequencing and assembly data: <i>Amazona aestiva</i>	This paper	GenBank: LMAW00000000
Genome annotation: <i>Amazona aestiva</i>	This paper	GenBank: LMAW01000000
Genome assembly and annotation: <i>Amazona vittata</i>	NCBI	BioProject: PRJNA171587
Genome assembly and annotation: <i>Anas platyrhynchos</i>	NCBI	BioProject: PRJNA46621
Genome assembly and annotation: <i>Ara macao</i>	NCBI	BioProject: PRJNA175470
Genome assembly and annotation: <i>Balearica regulorum gibbericeps</i>	NCBI	BioProject: PRJNA212879
Genome assembly and annotation: <i>Calypte anna</i>	NCBI	BioProject: PRJNA212866
Genome assembly and annotation: <i>Chaetura pelagica</i>	NCBI	BioProject: PRJNA202089
Genome assembly and annotation: <i>Charadrius vociferus</i>	NCBI	BioProject: PRJNA212867
Genome assembly and annotation: <i>Colinus striatus</i>	NCBI	BioProject: PRJNA212892
Genome assembly and annotation: <i>Columba livia</i>	NCBI	BioProject: PRJNA167554
Genome assembly and annotation: <i>Cuculus canorus</i>	NCBI	BioProject: PRJNA212869
Genome assembly and annotation: <i>Egretta garzetta</i>	NCBI	BioProject: PRJNA232959
Genome assembly and annotation: <i>Eurypyga helias</i>	NCBI	BioProject: PRJNA212893
Genome assembly and annotation: <i>Falco peregrinus</i>	NCBI	BioProject: PRJNA159791
Genome assembly and annotation: <i>Gallus gallus</i>	NCBI	BioProject: PRJNA13342
Genome assembly and annotation: <i>Haliaeetus leucocephalus</i>	NCBI	BioProject: PRJNA237821
Genome assembly and annotation: <i>Manacus vitellinus</i>	NCBI	BioProject: PRJNA212872
Genome assembly and annotation: <i>Meleagris gallopavo</i>	NCBI	BioProject: PRJNA62397
Genome assembly and annotation: <i>Melopsittacus undulatus</i>	GigaDB	GigaDB Accession: 1985454
Whole brain transcriptome data: <i>Melopsittacus undulates</i>	NCBI	SRA Accession: SRR029329–30
Whole brain transcriptome data: <i>Melopsittacus undulatus</i>	GigaDB	GigaDB Sample: GK0K2XF01
Genome assembly and annotation: <i>Nestor notabilis</i>	NCBI	BioProject: PRJNA212900
Genome assembly and annotation: <i>Nipponia nippon</i>	NCBI	BioProject: PRJNA232572
Genome assembly and annotation: <i>Pelecanus crispus</i>	NCBI	BioProject: PRJNA212901
Genome assembly and annotation: <i>Opisthocomus hoazin</i>	NCBI	BioProject: PRJNA212873
Genome assembly and annotation: <i>Phalacrocorax carbo</i>	NCBI	BioProject: PRJNA212903
Genome assembly and annotation: <i>Picoides pubescens</i>	NCBI	BioProject: PRJNA212874
Genome assembly and annotation: <i>Podiceps cristatus</i>	NCBI	BioProject: PRJNA212905
Genome assembly and annotation: <i>Struthio camelus australis</i>	NCBI	BioProject: PRJNA212875
Genome assembly and annotation: <i>Taeniopygia guttata</i>	NCBI	BioProject: PRJNA122047
Genome assembly and annotation: <i>Tyto alba</i>	NCBI	BioProject: PRJNA212909
AnAge database of animal lifespan data	Tacutu et al., 2013 [15]	http://genomics.senescence.info/species/

(Continued on next page)

Continued

REAGENT or RESOURCE	SOURCE	IDENTIFIER
GenAge database of experimental longevity data	Tacutu et al., 2013 [15]	http://genomics.senescence.info/genes/
Structure of the catalytic subunit of telomerase, <i>TERT</i> , <i>Tribolium castaneum</i>	Protein Data Bank	PDB: 3DU6
Ultra-conserved noncoding element (UCNE) sequences, <i>Gallus gallus</i>	Dimitrieva and Bucher 2013 [29]	https://ccg.vital-it.ch/UCNEbase/
Vertebrate gene sequence database	GenBank (release 208)	https://www.ncbi.nlm.nih.gov/genbank/
Software and Algorithms		
Paired end adaptor trimming, filtering	SeqPrep	https://github.com/jstjohn/SeqPrep
Mate pair adaptor trimming, filtering	NxTrim	https://github.com/sequencing/NxTrim
Sequencing error correction	Quake	http://www.cbc.umd.edu/software/quake/
Genome assembly	AllPaths-LG	http://software.broadinstitute.org/allpaths-lg/blog/?page_id=12
Genome assembly	ABYSS	http://www.bcgsc.ca/platform/bioinfo/software/abyss
Genome assembly	Meraculous	https://jgi.doe.gov/data-and-tools/meraculous/
Intra-scaffold gap-filling	GapFiller	https://www.baseclear.com/bioinformatics-tools/
Genome sequence alignment	Exonerate	https://www.ebi.ac.uk/about/vertebrate-genomics/software/exonerate
Gene prediction	AUGUSTUS	http://bioinf.uni-greifswald.de/augustus/
Genome annotation	SABIA	http://www.sabia.lncc.br
Gene pathway analysis	KEGG	http://www.genome.jp/kegg/
Gene orthology classification	COG	https://www.ncbi.nlm.nih.gov/COG/
Predicted protein domain analysis	InterPro	http://www.ebi.ac.uk/interpro
Pairwise sequence alignment	BLAST	https://blast.ncbi.nlm.nih.gov/Blast.cgi
Gene clustering	JVenn	http://jvenn.toulouse.inra.fr/app/example.html
miRNA discovery	miRDeep	https://github.com/rajewsky-lab/mirdeep2
miRNA validation	miRBase	http://www.mirbase.org/
miRNA analysis	RNAfold	https://www.tbi.univie.ac.at/RNA/RNAfold.1.html
Repetitive & low complexity sequence analysis	RepeatMasker	http://www.repeatmasker.org/
Transposable element discovery	MITE-hunter	http://target.iplantcollaborative.org/mite_hunter.html
Sequence alignment visualization and editing	Jalview v2	http://www.jalview.org/
Transposable element filtering and processing	'One code to find them all' perl tool	http://doua.prabi.fr/software/one-code-to-find-them-all
Microsatellite marker analysis	QDD v3.1	http://net.imbe.fr/~emeglecz/qdd.html
Clustering gene ortholog groups	OrthoMCL	http://orthomcl.org/orthomcl/
Phylogenetically aware multiple sequence alignment	PRANK	http://wasabiapp.org/software/prank/
Sequence substitution rate evolution analysis	PAML	http://abacus.gene.ucl.ac.uk/software/paml.html
Gene functional annotation clustering	DAVID 6.8	https://david.ncifcrf.gov/
Phylogenetic tree construction	PhyML	http://www.atgc-montpellier.fr/phyml/
Protein structure visualization	Jmol	http://jmol.sourceforge.net
Gene sequence alignment	BLAT	http://hgdownload.soe.ucsc.edu/admin/exe/
Gene alignment manipulation	BEDOPS	https://github.com/bedops/bedops
Transcriptome read trimming	Trimmomatic	http://www.usadellab.org/cms/?page=trimmomatic
Transcriptome read indexing	Bowtie2	http://bowtie-bio.sourceforge.net/bowtie2/index.shtml
Transcriptome read alignment	Tophat2	https://ccb.jhu.edu/software/tophat/index.shtml
Transcriptome read manipulation	SAMtools	http://www.htslib.org/
Statistical computing software	R	https://cran.r-project.org/
Phylogenetically aware statistical analyses	GEIGER v 2.0.6	https://cran.r-project.org/web/packages/geiger/index.html

CONTACT FOR REAGENT AND RESOURCE SHARING

Further information and requests for resources and reagents should be directed to and will be fulfilled by the Lead Contact, Claudio V. Mello (melloc@ohsu.edu).

EXPERIMENTAL MODEL AND SUBJECT DETAILS

The Blue-fronted Amazon, *Amazona aestiva*, individual whose genome was sequenced is alive as of the writing of this paper. The individual is an adult male, born in captivity in 2003 in the Vale Verde Ecological Park in Betim, Minas Gerais, Brazil, under register number FVVF132, and tissue voucher B04212 deposited at Centro de Coleções Taxonômicas of Universidade Federal de Minas Gerais. His parents were obtained in southern Brazil, where subspecies *A. aestiva xanthopteryx* is commonly found. Blood for whole genome sequencing was collected in 2013 through brachial venipuncture according to protocol 202/2007, approved by CEUA-UFMG (Comissão de Ética no Uso de Animais - Ethics Committee for Animal Use in Research at the Federal University of Minas Gerais).

METHOD DETAILS

Genome Sequencing

About 600 μ l of whole blood for genomic DNA was collected in heparinized capillary tubes, promptly mixed with EDTA 50 mM 1:1 (v/v), and kept in ice until DNA extraction. DNA was extracted using DNeasy Blood & Tissue Kit (QIAGEN), according to manufacturer's instructions; 10 μ l of the blood/EDTA solution was used as starting input material. DNA integrity was checked by electrophoresis in 0.8% agarose gel and quantified by spectrophotometry using a Nanodrop 2000C.

The 1.126 gigabase genome of the Blue-fronted Amazon was sequenced using high-coverage Illumina and 454 technologies to 117.59x and 3.1x coverage, respectively. Four Illumina libraries were generated for sequencing: two paired-end with an insert size of 300 bp; and two mate-paired libraries, with estimated insert sizes of \sim 1.4 kb and \sim 4 kb. Fourteen single-end 454 libraries, with a mean read length of 493 bp, were also sequenced. The Illumina paired-end sequencing data was filtered for low read quality and adaptor trimmed with SeqPrep (<https://github.com/jstjohn/SeqPrep>). Mate pair libraries were adaptor trimmed and identified using Illumina's NxTrim (<https://github.com/sequencing/NxTrim>). Reads were corrected by most frequent kmers by Quake (<http://www.cbcb.umd.edu/software/quake/>). The initial genome assembly was performed using all four Illumina libraries with AllPaths-LG with all filtering and correction parameters selected (http://software.broadinstitute.org/allpaths-lg/blog/?page_id=12). The $n = 14$ 454 libraries were incorporated by means of intra-scaffold gap filling with GapFiller (<http://www.baseclear.com/bioinformatics-tools/>). An additional round of gap-filling was performed using the Illumina 5 kb library with GapFiller. We also explored other approaches of combining the different libraries using different assemblers, such as ABySS (<http://www.bcgsc.ca/platform/bioinfo/software/abyss>) and Meraculous (<https://jgi.doe.gov/data-and-tools/meraculous/>), but determined the current approach produced the best result based on various metrics of contiguity and completeness. The resultant assembly (Aaes1) contains 3,232 scaffolds with a scaffold N50 size of 1.09 Mb and a contig N50 size of 27.8 kb (Table S3). Using BLASTn (<https://blast.ncbi.nlm.nih.gov/Blast.cgi>), Blue-fronted Amazon scaffolds were mapped to the genomes of chicken and zebra finch for additional comparative genomic analysis (Figure S3).

Genome Annotation

We generated *in silico* gene predictions through a combination of reference-guided and *ab initio* procedures. Exonerate (<https://www.ebi.ac.uk/about/vertebrate-genomics/software/exonerate>), a tool developed to predict genes by sequence alignment using proteins or transcripts from related organisms to the genome of interest, was implemented for reference-guided gene prediction, using as reference set the Ensembl 74 protein models from chicken (*Gallus gallus*, galGal4). This set of reference genome protein models was aligned to the Blue-fronted Amazon scaffold assembly using Exonerate protein2genome with a minimum 40% identity. A gene feature format file (.gff) containing gene predictions was generated from the Exonerate alignments. To generate gene predictions in the Blue-fronted Amazon scaffold assembly based on gene structural features, we used AUGUSTUS (<http://bioinf.uni-greifswald.de/augustus/>), an *ab initio* gene predictor that learns to identify genes based on structural similarity to genes provided in a training set. The AUGUSTUS-generated gene predictions were built using known gene models from chicken as a training set (provided by the AUGUSTUS package), which were corroborated with the alignment-based predictions produced by Exonerate (converted from .gff to .hints format for use in AUGUSTUS). Predictions were guided by, but not constrained to, the homology evidence generated by Exonerate, allowing for the prediction of novel genes unidentifiable through reference-guided approaches. Predictions in repetitive regions were minimized by using a softmasked version of the genome for gene prediction and the softmasking parameter of AUGUSTUS. We excluded within AUGUSTUS gene predictions with in-frame stop codons, returning only complete gene models with start and stop codons. We used SABIA (<http://www.sabia.lncc.br>), an automated annotation pipeline, to annotate all gene predictions with an open reading frame (ORF), taking into account BLAST similarity to sequences in various databases, including the KEGG orthology (KO, <http://www.genome.ad.jp/kegg>) and Cluster of Orthologous Groups (COG, <http://www.ncbi.nlm.nih.gov/COG/>) databases, the presence of predicted protein motifs using InterPro (<http://www.ebi.ac.uk/interpro/>), and Gene Ontology (GO, <http://geneontology.org/>).

We performed blastp searches to identify orthologs of Blue-fronted Amazon gene predictions among the complete protein sets of chicken, zebra finch, budgerigar, and kea. Using the Blue-fronted Amazon predicted proteins as query, we considered as orthologs BLAST alignments which corresponded to best hits with an e-value < 1e-10, and both query and subject coverage > 60%. Using JVenn (<http://bioinfo.genotoul.fr/jvenn/example.html>) we clustered genes from the other four birds that were the best hit for the same Blue-fronted Amazon gene prediction.

The *ab initio* and reference-based gene prediction methodologies used to annotate the Blue-fronted Amazon genome (Exonerate and AUGUSTUS) yielded a combined total of 16,200 gene predictions. 12,839 of these represented open reading frames (ORFs) containing both start and stop codons, which were validated and annotated using SABIA. BLAST analysis against chicken, zebra finch, budgerigar, and kea assemblies identified 11,094 presumed orthologs, with 7,692 present in all 5 genomes (Complete list of gene predictions with orthology information in Data S1A).

In order to find microRNA (miRNA) precursors orthologous to those found in chicken and zebra finch we used mirDeep (<https://github.com/rajewsky-lab/mirdeep2>) and RNAfold (<https://www.tbi.univie.ac.at/RNA/RNAfold.1.html>). 1,230 mature microRNAs from chicken and zebra finch were retrieved from the miRBase database (<http://www.mirbase.org/>) and used as queries against the Blue-fronted Amazon genome with mirDeep, using default parameters. The miRNA genome hits were retrieved and the secondary structure solved with RNAfold. Solved secondary structures were filtered to include minimum free energy < 10 kcal/mol, no more than three gaps of 3 to 4 nt in length, two of 5 nt, or one of length 6 to 8 nt. The resulting sequences were considered to be putative microRNA precursors. We predicted 86 miRNA precursors, belonging to 70 different miRNA families (Data S1B).

We conducted a survey of the repetitive content of the Blue-fronted Amazon genome for sequences falling into two distinct categories: transposable elements (TEs) and tandem repeats (i.e., microsatellites). TEs were identified through a combination of *de novo*, homology-based, and structure-based prediction methodologies. The homology-based approach involved searching the Blue-fronted Amazon genome for expansions of known TEs using publicly available databases, as follows. We used RepeatMasker (<http://www.repeatmasker.org/>) to identify elements similar to other known TEs in Repbase 19.06, using -species = aves. RepeatMasker was also used for estimating the amount of small RNAs, satellite DNA, low complexity regions, and simple repeats. To identify and classify parrot-specific repetitive elements, we employed RECON and RepeatScout, two *de novo* repeat finding packages invoked from within the RepeatModeler package, using default parameters (<http://www.repeatmasker.org/>). To predict candidate miniature inverted-repeat transposable elements (MITEs), we used MITE-hunter (http://target.iplantcollaborative.org/mite_hunter.html) with default parameters. The sequence alignments obtained by MITE-hunter were manually checked and edited in Jalview v2 (<http://www.jalview.org/>). All consensus output from RepeatModeler and MITE-Hunter was used to build a library in RepeatMasker, which was run again to find additional examples of these elements in the Blue-fronted Amazon genome. In order to accurately determine the number of TE copies found, including reconstruction of full-length copies, we applied the 'One code to find them all' perl tool (<http://doua.prabi.fr/software/one-code-to-find-them-all>) to parse the .out files obtained from the RepeatMasker analyses. The final results obtained from this analysis for each of the three tools (RepeatMasker, RepeatModeler and MITE-Hunter) were combined, removing redundancies. Finally, we identified TE units, which consisted of genomic regions containing contiguous TE predictions obtained by all three tools, which could be complete, incomplete, or nested TEs. These were classified as retrotransposons (Class I TEs) or DNA transposons (Class II TEs). TE units identified by more than one tool, but that did not fit within these categories, were designated unclassified TEs.

The combined TE count identified by three prediction methods (homology-based RepBase searches in RepeatMasker and *de novo* searches in RepeatModeler and MITE-hunter) totaled 267,799, representing 138.2 Mb or 12.23% of the Blue-fronted Amazon genome assembly (Table S4). Inclusion of small RNAs, satellites, low complexity regions, and simple repeats raise this total to 13%. The majority of TE predictions were categorized as long interspersed nuclear elements (LINEs; 7.14% of the total genome assembly), followed by unclassified TEs (2.38%), miniature inverted-repeat transposable elements (MITEs; 2.06%), long terminal repeats (LTRs; 0.64%), short interspersed nuclear elements (SINEs; 0.01%), and other DNA transposon families (0.02%).

Selection of microsatellite markers and primers was performed using QDD v3.1 (<http://net.imbe.fr/~emeglecz/qdd.html>) with default parameters, which filtered candidate markers based on similarity to known transposable elements in order to increase the genotyping success rate. We first identified 3,754 candidate microsatellite loci excluding 238 loci that overlapped with subsequently identified TEs resulted in a final count of 3,516 microsatellite loci in 1,040 different scaffolds, containing from 5 to 29 repeats. Of these, 2,775 were found to represent dinucleotide microsatellite loci, followed by smaller proportions of trinucleotide, tetranucleotide, pentanucleotide, and hexanucleotide loci, in this order. For each locus we also identified primers designed to generate amplicons varying between 90 and 300 bp for use in population genetics studies (Data S1C).

Longevity

Protein and CDS sequences from 22 birds in addition to Blue-fronted Amazon (Table S1) were retrieved from the GigaScience repository associated with the Avian Phylogenomics Consortium [11]. These species reflect a wide range of phylogeny [11] and were selected based on the availability of annotated genomes and reliable maximum longevity data, either from wild or controlled captive conditions, which were obtained from the AnAge database [15]. We note that lifespan data meeting the threshold for inclusion in the study were not available in the AnAge database for any songbirds with an available genome assembly, including zebra finch.

These birds were divided into two groups: regular-longevity (RL, when maximum observed longevity was lower than or comparable to maximum predicted longevity based on body mass) and high-longevity (HL, when maximum observed longevity was at least

20% higher than maximum predicted longevity, see Table S1). To infer expected longevity, we treated separately birds where longevity data derived from captive versus wild birds. We used the formulas $Ac = 5.07 \pm 1.63 \times W^{0.23 \pm 0.02}$ (where Ac is age in years for captive birds and W is weight in grams) and $Aw = 4.75 \pm 1.55 \times W^{0.17 \pm 0.01}$ (where Aw is age in years for wild birds) as formulated by Prininger [12]. Adult weight was extracted from AnAge [15].

The complete set of protein sequences from all 23 bird species analyzed was used in a blastp search and clustered with orthoMCL (<http://orthomcl.org/orthomcl/>) generating 22,380 clusters. Of these, 4,132 represented single-gene ortholog clusters (SGOs), with no more than one copy in each of the 23 bird species. In order to infer the level of selective pressure acting on longevity gene sets, phylogenetically aware CDS alignments were generated by PRANK (<http://wasabiapp.org/software/prank/>), rooted with a tree obtained from the Avian Phylogenomics data [11]. To assess ratios of nonsynonymous (dn) to synonymous (ds) substitution rates we implemented branch-sites test of selection using codeml from the PAML (Phylogenetic Analysis by Maximum Likelihood) package (<http://abacus.gene.ucl.ac.uk/software/paml.html>), rooted with the same avian tree as before. For all models, codeml was run with the following parameters: runmode = 0, Codonfreq = 2, kappa = 3, omega = 0.2, fix_alpha = 1. For the null model control file (no selection in HL birds relative to RL birds) we specified model = 0, whereas for the alternative model (differential selection in HL birds relative to RL birds) we specified model = 2. To identify genes under selection in HL birds, the likelihood values of the two models were compared using a likelihood ratio test (LRT, p value < 0.01, degrees of freedom = 1), and differential dn/ds (ω) values of HL versus RL birds were obtained to identify the direction of selection. Proteins predicted to be under significantly differential selective pressure were manually inspected and suspect protein predictions representing partial or artifactual gene models were removed from subsequent analyses. The complete list of genes under significant selection in HL birds relative to RL birds, ranked by differential ω (HL-RL), is presented in Data S1D. In general, dn/ds means were small, indicating strong purifying selection acting on these genes (62.5% and 82.6% ≤ 0.2 for HL and RL, respectively). Genes with divergent selection in long-lived birds were grouped into gene ontology (GO) functional annotation clusters using DAVID 6.8 (<https://david.ncicfcr.gov/>) (Table S2).

The dn/ds analyses considered all codon sites in protein-coding sequences. As a complementary test of differential selective pressure at specific sites, SGOs were analyzed with a site model implemented in codeml (<http://abacus.gene.ucl.ac.uk/software/paml.html>), comparing the likelihood values of a neutral (runmode = 0, model = 0, and NSites = 1) against a positive selection model (runmode = 0, model = 0, and NSites = 2) with LRT (p value < 0.01, degrees of freedom = 2). Phylogenetic trees were constructed with PHYML (<http://www.atgc-montpellier.fr/phyml/>). The posterior probabilities of positively selected sites were estimated with Bayes Empirical Bayes (BEB) with $\alpha = 0.05$. InterProScan 5 (<http://www.ebi.ac.uk/interpro/interproscan.html>) was used to annotate positively selected sites that correspond to residues located within discrete functional domains (Data S1E).

For the protein structural analysis of the catalytic domain of *TERT*, a model derived from *Tribolium castaneum* was used (Protein Data Bank ID: 3DU6). A multiple alignment was performed with PRANK to determine the residues corresponding to those with evidence of positive selection in the avian high longevity group. The Jmol visualizer (www.jmol.org/) was used to load and manipulate the PDB files, highlighting the position of selected residues.

Novel Genes

We sought to identify novel genes common to all parrots – and present in no other species – that arose from parent genes through gene duplication events or *de novo* through other mechanisms, and which could explain some aspects of psittacine biology. We searched for parrot novel genes using two complementary but separate strategies. The first strategy, based on sequence identity, was to manually examine the set of 1,822 Blue-fronted Amazon gene predictions for which no KEGG orthology group could be assigned during gene annotation. The second, based on gene synteny, was to employ a custom ‘locus-based’ strategy to identify gene predictions in the Blue-fronted Amazon genome that did not overlap with alignments of orthologous genes from chicken and zebra finch. For the second approach, we initially identified orthologous loci in the Blue-fronted Amazon genome by aligning, in independent analyses, the complete sets of chicken and zebra finch models from Ensembl 80 using BLAT (<http://hgdownload.soe.ucsc.edu/admin/exe/>), optimizing parameters to maximize model alignment while minimizing artifactual mappings (stepSize = 3, maxNtSize = 200000, repMatch = 2253, minScore = 100, minIdentity = 0), and retaining only the best alignment of each query using psiReps (parameters: noIntrons, singleHit, minAli = 0). Chicken and zebra finch were chosen as background species as they represent the non-parrot avian species with the most complete genomes and best-supported gene annotations, as well as representing the major Neoaves and Galloanseriforme lineages of birds (parrots belong to Neoaves). Blue-fronted Amazon gene predictions that significantly overlapped with the orthologous loci in these two other species were removed using BedOPS (<https://github.com/bedops/bedops>); the remaining predictions were considered candidate novel genes. The combined novel gene predictions from both approaches and subtracting species were filtered to remove predictions likely to represent artifactual models or retroviral elements (BLAT score < 100, score/span ratio ≥ 0.7). Using this ‘locus-based’ approach, we identified 2,416 gene predictions in the Blue-fronted Amazon that were non-overlapping with non-parrot ortholog alignments.

After filtering to exclude small, low-scoring predictions and partial or compacted predictions likely to represent alignment artifacts, we performed extensive multi-species alignments and manual synteny verification to validate or exclude novel gene predictions (i.e., shared synteny in Blue-fronted Amazon, budgerigar, and kea; and present in no other avian or non-avian genomes). We first performed a blastp alignment of all novel gene predictions against the NCBI non-redundant protein sequence database, excluding predictions that returned significant hits in non-parrot species. This database represents over 68 million unique protein sequence predictions submitted to GenBank, including over 60 avian species to date (GenBank release 208). As a further exclusionary step, those predictions that were not excluded through the BLAST alignment were aligned to two distantly related parrot

species (budgerigar, Kea) and outgroup species (zebra finch, Peregrine Falcon, chicken, American alligator, Anole lizard, and human) using BLAT with sensitized parameters optimized for these cross-species alignments, in order to confirm the presence of orthologous novel genes in all parrots and absence in non-parrots. This exhaustive validation step has been previously shown to be necessary for accurate novel gene prediction and exclusion of orthologs that may be partially sequenced, highly divergent, or unpredicted and thus not represented in NCBI's sequence databases [14].

We note that synteny verification is a critical factor in maximizing the effectiveness of orthology determination, largely because BLAT or BLAST alignments, even when performed mutually and recursively, often cannot discriminate across paralogous genes and/or closely related members of the same gene family. Synteny verification is also particularly useful in situations (e.g., due to genomic gaps) when only a fragment of a gene is present and shows similar partial cross alignments to queries from multiple members of the same gene family. As previously discussed [14], this step is performed manually, by verifying across multiple species the flanking genes of search alignment hits for a given query. A gene is considered novel (*de novo*) or a novel paralog within a given species (or clade) when it is present in that species (or group) but fails to align at that same syntenic context in any other species (or clade); conversely, a gene is only considered the correct ortholog if there is evidence of alignment to the same syntenic context in other species and outgroups. Failure to utilize synteny criteria results in the frequent misidentification of orthologs, which confounds the correct classification of novel genes in a given species. As we took a conservative stance in excluding models where shared gene synteny in parrots could not be confirmed, ours is likely an underrepresentation of the true set of parrot-specific genes.

To further validate these predictions, we performed a brain transcriptome analysis to determine whether there is any evidence of expression of parrot novel genes. Given the unavailability of high-quality brain tissue from the Blue-fronted Amazon, a species protected by CITES (Convention on the Trade of Endangered Species), the expression of conserved parrot novel genes was assessed using the complete set of brain transcriptome data available from budgerigar.

The total brain transcriptomes of 3 male budgerigars were retrieved from NCBI (SRA Accession: SRR029329–30) and GigaDB (sample ID: GK0K2XF01). Trimmomatic (<http://www.usadellab.org/cms/?page=trimmomatic>) was used for adaptor trimming as well as trimming of low-quality sequence. Only reads with length > 30 bp were retained. An index of the budgerigar genome was built using bowtie2 (<http://bowtie-bio.sourceforge.net/bowtie2/index.shtml>), and budgerigar transcriptome reads were mapped onto the budgerigar genome using tophat2 with the default recommended parameters (<https://ccb.jhu.edu/software/tophat/index.shtml>). Mapped reads were selected using SAMtools (<http://www.htslib.org/>). All non-uniquely mapped reads were removed, so that expression among closely related genes could be distinguished. Evidence of gene expression was assessed in terms of counts of reads wholly or partially mapped to exons of budgerigar gene models, or overlapping with such reads.

In order to investigate potential gene function, parrot novel gene predictions were subsequently characterized in terms of their predicted protein domains. Protein sequences were annotated using InterProScan 5 (<http://www.ebi.ac.uk/interpro/interproscan.html>), retrieving domain information from multiple publicly available databases including PROSITE, Pfam, PRINTS, ProDom, SMART, and PANTHER. Sequences were further annotated through searches against NCBI's conserved domains database (<https://www.ncbi.nlm.nih.gov/Structure/cdd/cdd.shtml>) and blastp alignments to NCBI's GenBank sequence database (release 208, <https://www.ncbi.nlm.nih.gov/genbank/>) to identify potential related genes in other species that could provide clues to gene family membership.

We identified several categories of high-confidence novel protein-coding genes that could be found exclusively in parrot genomes. A small subset of novel genes ($n = 12$; Table 1, Data S1F) were single paralogs of an orthologous parent gene. For two of the genes, PSMD6 and DESI2, the duplicated copies are located at sites of syntenic disruption that are indicative of chromosomal rearrangements, suggesting their origination resulted from a breakpoint duplication event (Figures S1A and S1B). The fact that both copies in parrots share partial synteny with the parent gene in non-parrot genomes precludes a clear ortholog / duplicate distinction. It was also not possible to determine if the duplications resulted from intra- or inter-chromosomal rearrangements, as the Blue-fronted Amazon and budgerigar scaffolds have not yet been assembled into chromosomes. For the rest of the genes in this subset (Table 1), we could unambiguously identify the parent gene ortholog that gave rise to the parrot-specific gene duplication by establishing conserved synteny of an ortholog in parrot and non-parrot genomes, and the presence of a novel paralog at a syntenic location unique to parrot genomes. None of these novel paralogs could be found in any non-parrot genomes, including the genomes of songbirds. In some cases the duplication was partial, as only one or few domains present in the parent gene could be seen in the duplicated copy, for example, PLXNC1L compared to PLXNC1 (Figure S1C).

A further subset of novel genes represented expanded gene families ($n = 10$ family expansions; Table 1, Data S1G): these are genes that have undergone extensive duplication at multiple syntenic locations in parrot genomes, whereas only a single copy can be readily identified in non-parrot genomes. For six of these gene family expansions, we were able to infer function, discussed in the paper, based on predicted conserved domains and cross-alignments to NCBI sequence databases. Other gene expansions had no predicted conserved protein domains or significant BLAST alignments that could provide clues as to molecular function. A distinct subset were found to contain viral / retrotransposon-like elements, suggesting they largely represent retrotransposon-mediated expansions. Since these predictions are not present in non-parrot genomes, they seem to represent parrot specific viral-related expansions.

In addition to genes with clear gene family relationships, we have also discovered a large set ($n = 136$; Table 1, Data S1H) of novel gene predictions unique to parrots that appear to represent *de novo* novel genes without a parent ortholog in any species. RNA-seq data confirm brain expression for a subset of these predictions (Data S1H1; $n = 17$, 12%), supporting their validity but also indicating a link to brain function. Half of this brain-expressed set ($n = 8$) had either predicted protein domains (e.g., transmembrane domain or signal peptide suggestive of membrane localization or secreted peptide, respectively) and/or partial BLAST hits to genes of known

function (mostly enzymes) in other organisms, suggesting relations to those genes or functions. The other half ($n = 9$) did not have predicted domains or detectable BLAST hits to other genes. They likely do not represent false positive predictions, given their high conservation across parrot genomes. However, even though they had a predicted ORF, they might not be expressed as proteins and thus could represent long-noncoding RNAs, or even ‘proto-genes’ [28]. Growing evidence points to prominent roles of noncoding RNAs in gene expression regulation, and the expression of ‘pre-functional’ long-noncoding RNAs has also been suggested as a prerequisite for *de novo* novel gene evolution [28]. Distinguishing among the possibilities above will require further analyses of these brain-expressed novel transcripts, which would include assessment of expression at the protein level and/or examining possible transcriptional regulatory targets of noncoding RNAs.

Similarly, among novel predictions that lacked brain expression evidence, one subset had either predicted protein domains and/or partial BLAST hits to genes in other organisms (Data S1H2; $n = 27$, 20%), suggesting relations to other genes of known function. Additional subsets with no brain expression or predicted domains had either only very low-scoring BLAST hits (Data S1H3; $n = 45$, 33%), or no hits to non-parrot species (Data S1H4; $n = 47$, 35%), and thus their function and family relatedness are unclear. As with brain-expressed novel genes, these predictions may represent non-coding RNAs, but the lack of expression suggests that some could also be pseudogenes. The majority (73%) of these *de novo* novel gene variants showed substantial conservation across parrot species (> 70% cross-species BLAT alignment), indicating that they likely represent real genetic sequences unique to parrots.

A distinct set ($n = 34$; Data S1I) of novel gene predictions from the Blue-fronted Amazon could not be found in other species and thus may represent unique features of the Blue-fronted Amazon genome. This set included both single gene paralogs as well as gene family expansions. The majority of these contain predicted protein domains ($n = 21$, 62%) Some of these genes were not detected in budgerigar only, and could represent novel psittacine genes that were lost in budgerigar only, or alternatively they might be absent in budgerigar genome only due to sequence gaps in the current assembly of the latter. We were unable to distinguish these possibilities, due to the fragmentary nature of the current Kea, Scarlet Macaw, and Puerto Rican Parrot assemblies, which precludes the syntenic analysis necessary for accurate orthology determination.

Ultra-Conserved Noncoding Elements

4,351 UCNE consensus sequences from chicken were retrieved from UCNEbase (<https://ccg.vital-it.ch/UCNEbase/> [29]). Orthologous UCNEs were identified in Blue-fronted Amazon, as well as several parrot and non-parrot avian (outgroup) species where high-coverage genomes were available (zebra finch and chicken from Ensembl 80; Budgerigar, Kea, Golden-collared Manakin, Peregrine Falcon, Downy Woodpecker, Crested Ibis, Hoatzin, Pigeon, and Domestic duck from the GigaScience repository associated with the Avian Phylogenomics Consortium [11]), by aligning the chicken UCNE set to each genome using BLAST 2.2.31 with parameters `-blastn -dust no -evalue 0.01 -max_target_seqs 1 -max_hsps 1`. As UCNEs are defined as non-coding regions > 200bp with $\geq 95\%$ sequence identity between human and chicken, we considered UCNEs that exhibited a ratio of mismatches to total sequence length of 5% or more to be divergent. In order to identify UCNEs specifically divergent in the parrot lineage, we implemented the phylogenetic ANOVA in the R package GEIGER v 2.0.6 (<https://cran.r-project.org/package=geiger>), using the species tree from the avian phylogenomics consortium [11] and 1,000 *in silico* simulations. We thus identified 20 UCNEs that were significantly more divergent in parrots relative to other birds (phylogenetic ANOVA, $\alpha < 0.05$, Table S5). Syntenic gene position of each UCNE was checked manually; UCNEs where orthology across species could not be confirmed by shared synteny were removed from subsequent analyses.

QUANTIFICATION AND STATISTICAL ANALYSIS

To identify genes under selection in HL birds relative to RL birds, null versus alternate models of selection were compared using a likelihood ratio test (LRT, p value < 0.01, degrees of freedom = 1). To identify specific codon sites under selection in HL birds, a LRT was used to compare the likelihood values of a neutral against a positive selection model (p value < 0.01, degrees of freedom = 2; posterior probabilities of positively selected sites were estimated with Bayes Empirical Bayes with $\alpha = 0.05$). After identifying a set of UCNEs putatively divergent in parrots (ratio of mismatches 5% or more relative to chicken consensus sequence) we performed additional testing to confirm significant divergence in 3 parrots relative to 9 avian outgroup species using a phylogenetic ANOVA ($\alpha < 0.05$), using the species tree from the avian phylogenomics consortium [11] and 1,000 *in silico* simulations. All statistical tests were carried out in R (<https://cran.r-project.org/>).

DATA AND SOFTWARE AVAILABILITY

The genome assembly, associated raw sequence data, and gene predictions for the *Amazona aestiva* have been deposited in GenBank, EMBL-EBI, and DDBJ under the accession ID GenBank: LMAW00000000. The version described in this paper is version GenBank: LMAW01000000.

Current Biology, Volume 28

Supplemental Information

Parrot Genomes and the Evolution of Heightened Longevity and Cognition

Morgan Wirthlin, Nicholas C.B. Lima, Rafael Lucas Muniz Guedes, André E.R. Soares, Luiz Gonzaga P. Almeida, Nathalia P. Cavaleiro, Guilherme Loss de Moraes, Anderson V. Chaves, Jason T. Howard, Marcus de Melo Teixeira, Patricia N. Schneider, Fabrício R. Santos, Michael C. Schatz, Maria Sueli Felipe, Cristina Y. Miyaki, Alexandre Aleixo, Maria P.C. Schneider, Erich D. Jarvis, Ana Tereza R. Vasconcelos, Francisco Prosdocimi, and Claudio V. Mello

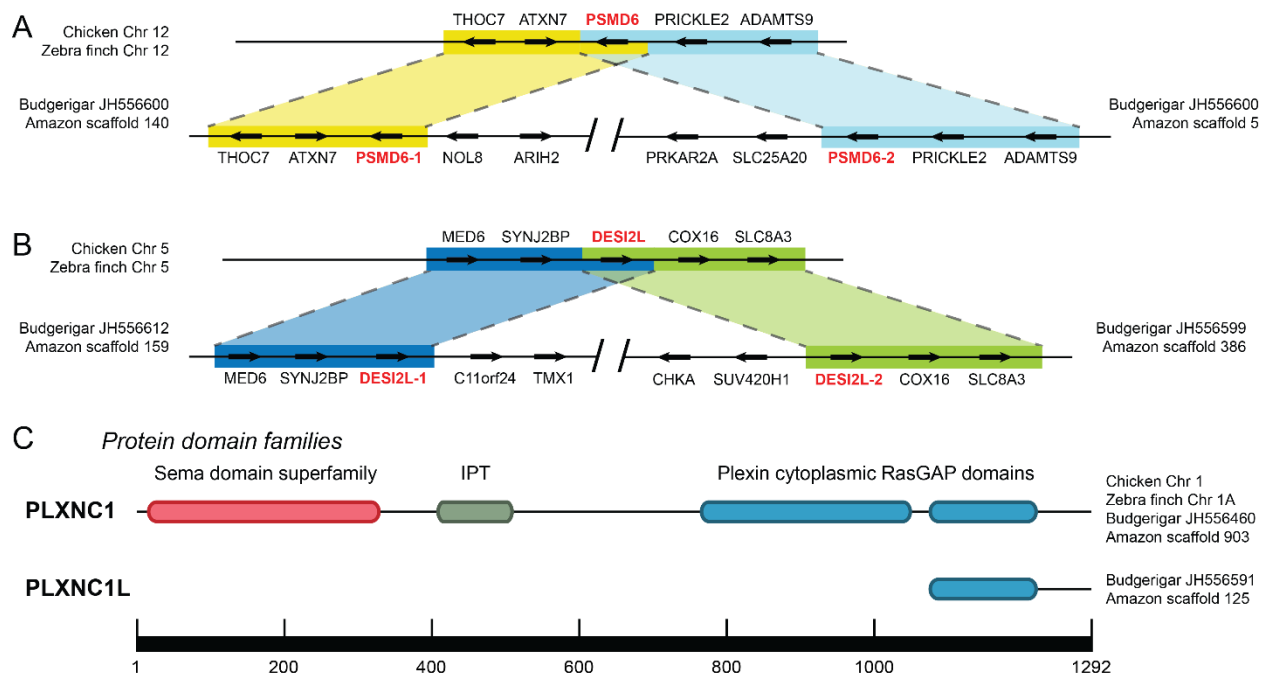


Figure S1. Novel gene duplications in parrots. Related to Table 1. (A-B) Depiction of chromosomal rearrangements unique to parrots and likely implicated in the generation of parrot-specific duplications of (A) PSMD6, a 26S proteasome subunit that colocalizes with DNA damage foci in cells that have suffered genotoxic damage, helping to ensure that these cells are targeted for senescence [S1], and (B) DESI2L, an apoptosis regulator and part of the early response to DNA damage [S2]. Further highlighting DNA repair and control of cell proliferation as important pathways in the evolution of parrots, several additional duplicated genes in parrots also regulate genomic stability and cell senescence: SUN2, which together with the known longevity factor SUN1 is part of the inner nuclear envelope and interacts with a DNA-dependent protein kinase (DNAPK) complex that functions in DNA nonhomologous end joining repair in response to DNA damage [S3]; SIDT1, implicated in intercellular transfer of siRNAs and the spread of chemoresistance in cancer [S4]; and MXRA7, member of a gene family involved in cell adhesion, matrix remodeling, cancer spread, and metastasis [S5]. (C) Alignment of conserved avian PLXNC1 and its parrot lineage-specific duplicate, PLXNC1L, depicting predicted protein domains. Numbers in scale indicate amino acid residue position in *A. aestiva* PLXNC1 ortholog. IPT, Immunoglobulin-like fold Plexin Transcription factors. See Table 1 for a summary and Data S1F-I for a complete list of novel genes duplicated and expanded in parrots.

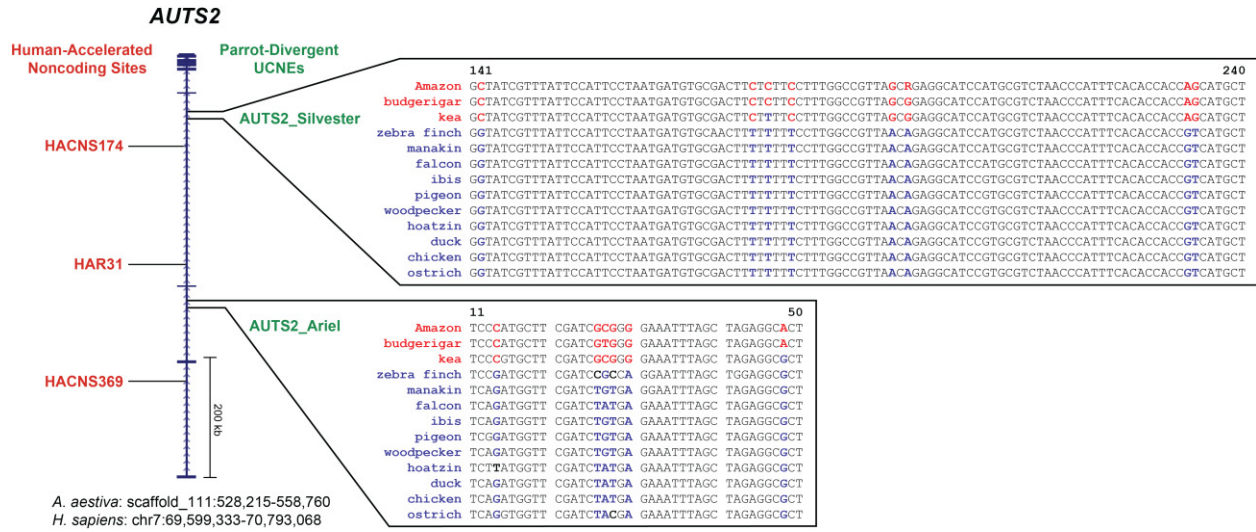


Figure S2. Parrot-specific divergence in ultra-conserved noncoding elements (UCNEs). Related to Table 2. Associated with AUTS2. Noncoding regions with evidence of accelerated evolution in the human lineage are indicated in red text at left (haCNS, human accelerated conserved noncoding sequences [S6]; HAR, human accelerated regions [S7]), and UCNEs with evidence of lineage-specific selection in parrots are indicated in green at right, with regions containing parrot-specific polymorphisms shown in the expansions at the far right. Multi-species sequence alignments of these regions reveal substitutions unique to parrots (in red) and non-parrot consensus polymorphisms (in blue). Numbers indicate nucleotide position within UCNEs. Further details and full list of UCNEs and associated genes divergent in parrots are described in STAR Methods: UCNEs.

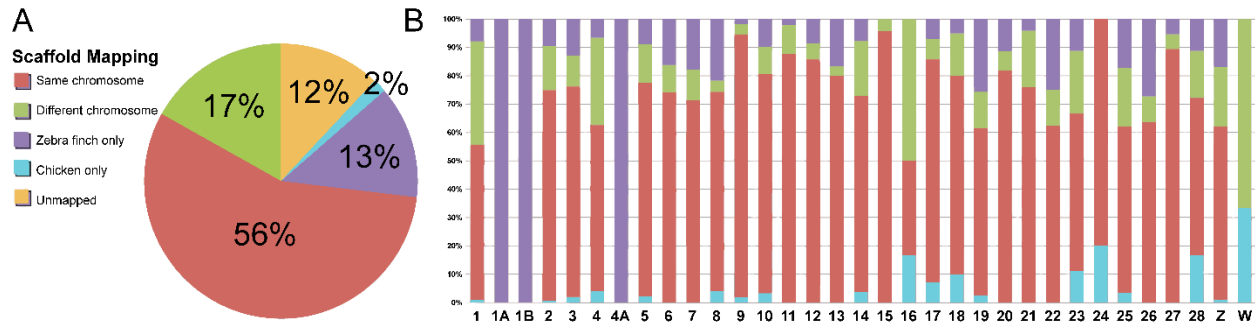


Figure S3. Comparative genomic analysis of Blue-fronted amazon and avian model species. Related to STAR Methods. Graphical depiction of *Amazona aestiva* scaffolds mapped onto the chicken and zebra finch genomes: A) scaffold mapping categories and corresponding percentages; B) chromosomal distribution of scaffold mapping categories.

Blue-fronted Amazon scaffolds were mapped to the genomes of chicken and zebra finch using blastn. Over half (56%) of the scaffolds mapped to the same chromosomes in both non-parrot species, indicating good conservation at the chromosome level (A, in red). Another considerable fraction of the scaffolds (17%) mapped to different chromosomes in the two non-parrot species (A, in green), likely reflecting inter-chromosomal rearrangements. The Blue-fronted Amazon genome shared more unique regions with zebra finch (13%) than with chicken (2%) (A, in purple and blue, respectively), consistent with their phylogenetic relationships [S8]. For the most part, individual chromosomes (depicted in B) showed comparable proportions of these different mapping categories. The few exceptions consisted of scaffolds mapping onto chromosomes that are lacking as a separate chromosomal unit in chicken (i.e. zebra finch chromosomes 1A, 1B, and 4A) or unsequenced in zebra finch (i.e. chromosome W).

We found that 12% of Blue-fronted Amazon scaffolds did not map to either chicken or zebra finch genomes (A, in orange). This corresponds to 1.1 Mb, 0.09% of the total genome sequence length. To rule out contamination by bacterial DNA a BLAST search was performed for highly similar sequences between these scaffolds and the entirety of the bacterial nucleotide database available at GenBank using an e-value cutoff of $1e-10$. None of the scaffolds had any significant alignment with bacterial sequences. Using the same approach, scaffolds that did not map to either genome were subsequently aligned to the genomes of the budgerigar, Kea, and Puerto Rican Parrot. All but 37 scaffolds (0.012% of the total genome sequence length) aligned to one or more of the other parrot genomes, suggesting that these 37 represent sequences specific to the Blue-fronted Amazon. Thus, the 12% of scaffold sequences uniquely found in parrots likely reflects true lineage-specific sequence divergence in this lineage.

Longevity group*	Species abbrev.	Species Name	Common Name	Adult weight (g)	Condition	Maximum Observed Longevity (years)	Maximum expected longevity**	Longevity Deviation (%)
RL	Bre	<i>Balearica regulorum</i>	Grey Crowned Crane	3372	Captivity	27.2	51.1	-46.8
RL	Can	<i>Calypte anna</i>	Anna's Hummingbird	4.4	Wild	8.5	8.2	3.7
RL	Cvo	<i>Charadrius vociferus</i>	Killdeer	88	Wild	10.9	14.1	-22.7
RL	Cst	<i>Colius striatus</i>	Speckled Mousebird	51	Captivity	11.5	17.9	-35.8
RL	Cca	<i>Cuculus canorus</i>	Common Cuckoo	111.5	Wild	12.9	14.7	-12.3
RL	Ppu	<i>Picoides pubescens</i>	Downy Woodpecker	25.6	Wild	11.9	11.3	5.3
RL	Ehe	<i>Eurypyga helias</i>	Sunbittern	210	Captivity	15	25.5	-41.2
RL	Gga	<i>Gallus gallus</i>	Red Junglefowl	779.8	Captivity	30	35.4	-15.3
RL	Hal	<i>Haliaeetus albicilla</i>	White-tailed Eagle	6696.5	Captivity	42	60.6	-30.7
RL	Hle	<i>Haliaeetus leucocephalus</i>	Bald Eagle	3175	Captivity	48	50.3	-4.6
RL	Mga	<i>Meleagris gallopavo</i>	Wild Turkey	6050	Wild	13	30.2	-57
RL	Nni	<i>Nipponia nippon</i>	Crested Ibis	1900	Captivity	25.8	44.2	-41.6
RL	Pcr	<i>Pelecanus crispus</i>	Dalmatian Pelican	9550	Captivity	35.3	66.2	-46.7
RL	Pca	<i>Phalacrocorax carbo</i>	Great Cormorant	3628.8	Wild	27.2	27.5	-1.1
RL	Pci	<i>Podiceps cristatus</i>	Great Crested Grebe	738.7	Wild	19.2	20.7	-7.3
RL	Sca	<i>Struthio camelus</i>	Ostrich	111000	Captivity	50	122.3	-59.1
HL	Aae	<i>Amazona aestiva</i>	Parrot	451	Captivity	49	30.9	58.6
HL	Cpe	<i>Chaetura pelagica</i>	Chimney Swift	22.8	Wild	15	11.1	35.1
HL	Cli	<i>Columba livia</i>	Rock Pigeon	358.7	Captivity	35	29.2	20
HL	Ega	<i>Egretta garzetta</i>	Little Egret	312	Wild	22.3	17.7	26
HL	Mun	<i>Melopsittacus undulatus</i>	Budgerigar	30	Captivity	21	15.7	33.8
HL	Nno	<i>Nestor notabilis</i>	Kea	867.5	Captivity	47	36.4	29.1
HL	Tal	<i>Tyto alba</i>	Common Barn Owl	580	Wild	34	19.8	71.7

Table S1. Lifespan data for wild and captive avian species. Related to Figure 1. List of avian species used in longevity analyses. *Longevity data were obtained from the AnAge database [S9], and are used as the basis for classification into regular-longevity (RL) or high-longevity (HL) groups. ** Estimated with $A(c)=5.07+-1.63xW^{0.23+-0.02}$ and $A(w)=4.75+-1.55xW^{0.17+-0.01}$, where A(c) is age in years for captivity birds, A(w) is age in years for wild birds, and W is weight in grams [S10].

Annotation Cluster 1: Enrichment Score: 4.12				
Annotation Category	Annotation Term	Count	p value	Benjamini
UP_KEYWORDS	Kinetochores	11	3.50E-06	5.80E-04
UP_KEYWORDS	Mitosis	17	4.10E-06	4.60E-04
UP_KEYWORDS	Centromere	12	1.10E-05	7.10E-04
GOTERM_BP_DIRECT	sister chromatid cohesion	11	1.20E-05	1.80E-02
UP_KEYWORDS	Cell division	20	1.30E-05	7.10E-04
GOTERM_BP_DIRECT	cell division	19	4.00E-05	3.10E-02
GOTERM_BP_DIRECT	mitotic sister chromatid segregation	6	5.90E-05	3.10E-02
UP_KEYWORDS	Cell cycle	25	9.70E-05	3.60E-03
GOTERM_CC_DIRECT	condensed chromosome kinetochores	9	1.00E-04	1.80E-02
GOTERM_BP_DIRECT	mitotic nuclear division	15	1.10E-04	4.30E-02
UP_KEYWORDS	Chromosome	18	2.10E-04	6.80E-03
GOTERM_CC_DIRECT	kinetochores	7	2.30E-03	1.90E-01
GOTERM_BP_DIRECT	chromosome segregation	4	1.10E-01	1.00E+00
Annotation Cluster 2: Enrichment Score: 2.61				
GOTERM_BP_DIRECT	mRNA splicing, via spliceosome	14	1.30E-04	4.20E-02
UP_KEYWORDS	mRNA processing	16	2.50E-04	7.60E-03
KEGG_PATHWAY	Spliceosome	10	7.60E-04	1.50E-01
GOTERM_CC_DIRECT	catalytic step 2 spliceosome	8	8.60E-04	9.90E-02
UP_KEYWORDS	mRNA splicing	13	8.60E-04	2.40E-02
UP_KEYWORDS	Spliceosome	8	3.90E-03	9.50E-02
GOTERM_MF_DIRECT	RNA binding	19	7.20E-03	6.90E-01
GOTERM_BP_DIRECT	RNA splicing	7	6.80E-02	1.00E+00
GOTERM_BP_DIRECT	mRNA processing	7	9.10E-02	1.00E+00
Annotation Cluster 3: Enrichment Score: 1.88				
GOTERM_CC_DIRECT	catalytic step 2 spliceosome	8	8.60E-04	9.90E-02
UP_KEYWORDS	Spliceosome	8	3.90E-03	9.50E-02
SMART	Sm	3	4.10E-02	9.50E-01
INTERPRO	Ribonucleoprotein LSM domain	3	4.70E-02	9.70E-01
INTERPRO	Like-Sm (LSM) domain	3	6.00E-02	9.80E-01
Annotation Cluster 4: Enrichment Score: 1.82				
GOTERM_BP_DIRECT	RNA processing	7	6.70E-03	7.00E-01
UP_KEYWORDS	Viral nucleoprotein	4	9.30E-03	1.90E-01
GOTERM_CC_DIRECT	viral nucleocapsid	4	1.10E-02	3.60E-01
UP_KEYWORDS	Ribonucleoprotein	11	1.90E-02	2.80E-01
GOTERM_CC_DIRECT	intracellular ribonucleoprotein complex	7	2.60E-02	5.30E-01
UP_KEYWORDS	Virion	4	3.70E-02	4.10E-01
Annotation Cluster 5: Enrichment Score: 1.63				
SMART	WD40	11	8.30E-03	6.90E-01
UP_SEQ_FEATURE	repeat:WD 3	11	1.20E-02	1.00E+00
UP_KEYWORDS	WD repeat	11	1.40E-02	2.20E-01
INTERPRO	WD40-repeat-containing domain	12	1.40E-02	1.00E+00
UP_SEQ_FEATURE	repeat:WD 6	9	1.40E-02	9.90E-01
UP_SEQ_FEATURE	repeat:WD 5	10	1.40E-02	9.60E-01
INTERPRO	WD40 repeat	11	1.40E-02	9.90E-01
UP_SEQ_FEATURE	repeat:WD 1	11	1.40E-02	9.30E-01

UP_SEQ_FEATURE	repeat:WD 2	11	1.40E-02	9.30E-01
UP_SEQ_FEATURE	repeat:WD 4	10	2.20E-02	9.70E-01
INTERPRO	WD40/YVTN repeat-like-containing domain	12	2.30E-02	9.90E-01
UP_SEQ_FEATURE	repeat:WD 7	5	2.20E-01	1.00E+00
INTERPRO	WD40 repeat, conserved site	4	5.20E-01	1.00E+00
Annotation Cluster 6: Enrichment Score: 1.43				
GOTERM_BP_DIRECT	kynurenine metabolic process	3	1.70E-03	3.30E-01
GOTERM_MF_DIRECT	kynurenine-oxoglutarate transaminase activity	3	1.70E-03	3.50E-01
INTERPRO	Pyridoxal phosphate-dependent transferase, major region, subdomain 2	4	2.50E-02	9.80E-01
INTERPRO	Aminotransferase, class I/classII	3	3.20E-02	9.60E-01
INTERPRO	Pyridoxal phosphate-dependent transferase	4	3.40E-02	9.50E-01
INTERPRO	Pyridoxal phosphate-dependent transferase, major region, subdomain 1	4	3.40E-02	9.50E-01
UP_KEYWORDS	Aminotransferase	3	4.60E-02	4.40E-01
GOTERM_MF_DIRECT	pyridoxal phosphate binding	4	7.60E-02	9.90E-01
UP_KEYWORDS	Pyridoxal phosphate	4	7.60E-02	5.60E-01
GOTERM_BP_DIRECT	biosynthetic process	3	9.40E-02	1.00E+00
KEGG_PATHWAY	Tryptophan metabolism	3	1.70E-01	9.60E-01
GOTERM_MF_DIRECT	catalytic activity	4	6.30E-01	1.00E+00
Annotation Cluster 7: Enrichment Score: 1.07				
UP_KEYWORDS	DNA damage	13	9.80E-03	1.80E-01
UP_KEYWORDS	Fanconi anemia	3	3.50E-02	4.00E-01
KEGG_PATHWAY	Fanconi anemia pathway	4	7.50E-02	9.30E-01
UP_KEYWORDS	DNA repair	7	3.20E-01	8.80E-01
GOTERM_BP_DIRECT	DNA repair	5	5.80E-01	1.00E+00

Table S2. Functional annotation of genes associated with increased longevity in birds. Related to Figure 2. Gene ontology (GO) functional categorization of genes where mean dn/ds values significantly differed between high- and regular-longevity birds (Bonferroni corrected p-value < 0.05). BP: biological process, MF: molecular function.

We identified TERT as a gene under strong selective pressure in HL birds relative to RL birds. While protective against cell senescence, a risk of high TERT activity is an increased rate of uncontrolled proliferation and tumor formation [S11]. Highlighting the importance of balancing these processes, we found genes under selective pressure in long-lived birds were enriched for processes related to cell proliferation and tumor suppression (Annotation Cluster 1). These include: BUB1B and BUB3, both mitotic checkpoint proteins that regulate the spindle assembly machinery during cell division and previously known longevity factors [S12]; KIF4A and KIF1BP, components of a microtubule-based motor protein that regulates cell division, proliferation, and cancer progression by controlling chromosome integrity during mitosis (overlapping in function with BUB genes) [S13]; and CCNE1, a member of the cyclin family implicated in cell cycling, chromosomal stability, and tumorigenesis [S14]. For complete set of genes under differential selection in HL versus RL birds please see Data S1D.

Species	Sequenced Genome Size	Sequencing depth – technology used	Number of scaffolds	N50 scaffold	N50 contig	Reference
Chicken	1.07 Gb	7x – Sanger	16,847	7.07 Mb	36 kb	[S15]
Zebra finch	1.2 Gb	6x – Sanger	37,422	10.4 Mb	39 kb	[S16]
Budgerigar	1.23 Gb	160x – Hybrid	25,212	10.6 Mb	55.6 kb	[S17, S18]
Puerto-Rican Parrot	1.18 Gb	24x – Illumina	148,255	19.2 kb	6.9 kb	[S19]
Scarlet Macaw	0.99 Gb	26x – Hybrid	192,790	16.0 kb	4.4 kb	[S20]
Kea	1.05 Gb	32x – Illumina	42,180	61.4 kb	26.5 kb	[S21]
Peach-faced Lovebird	1.12 Gb	100x – Illumina	52,900	118.3 kb	28.6 kb	[S22]
Blue-fronted Amazon	1.28 Gb	120.6x – Hybrid	3,128	1.09 Mb	27.8 kb	This study

Table S3. Assembly statistics for the Blue-fronted Amazon in the context of the initial releases of other avian genomes. Related to STAR Methods. The size of the *Amazona aestiva* draft genome assembly is similar to those of other high-coverage sequenced avian genomes, with 88% of the estimated genome size assembled with gaps and 82% without gaps. By comparison, the Puerto Rican Parrot, Scarlet Macaw, and Kea assemblies are much more discontinuous (148,255; 192,790; and 42,180 scaffolds, respectively [S19-21]), likely due to lower coverage, library insert sizes, and the longer 454 reads. Although the Illumina plus 454 assembled budgerigar genome has a higher N50 scaffold size statistic (10.6 Mb), that assembly is also split into substantially more scaffolds (25,212) with a larger range of fragment sizes and lower mean sequence length than the Blue-fronted Amazon assembly (44,319 bp and 349,524 bp, respectively) [S18]. *International Chicken Genome Consortium.

Transposable Element Class	RepeatMasker		RepeatModeler		MITE-Hunter		Total		Number of TE units
	bp	%	bp	%	bp	%	bp	%	
Retrotransposons									
SINEs	17,515	0.002%	48,504	0.004%	NA	NA	64,251	0.01%	187
LINEs	68,848,293	6.095%	33,069,485	2.927%	NA	NA	80,618,676	7.14%	122,178
LTR elements	3,142,254	0.278%	6,049,894	0.536%	NA	NA	7,195,515	0.64%	19,039
DNA transposons									
MITEs	3,756	0.000%	2,358	0.000%	23,227,765	2.06%	23,233,879	2.06%	26,317
Other	99,371	0.009%	71,263	0.006%	NA	NA	168,990	0.02%	800
Unclassified	4,203,118	0.372%	26,133,317	2.313%	15,249,652	1.35%	26,881,654	2.38%	99,278
Total	76,314,307	6.755%	65,374,821	5.787%	38,477,417	3.41%	138,162,965	12.23%	267,799

Table S4. Repeat content of the Blue-fronted Amazon genome. Related to STAR Methods. Numbers indicate length of repeats in base pairs (bp), their corresponding percentage of genome (%), and numbers of TE units.

The 12.23% total repetitive sequence content of the Blue-fronted Amazon genome at first appears substantially higher than in most other avian genomes. Previously the chicken and zebra finch repetitive sequences were initially reported at 8.5% [S15] and 7.7% [S16], respectively, and more recently similar figures were reported for other species [S20, S23]. The exception has been the Downy Woodpecker, where LINE content alone accounts for 18% of genomic sequence [S21]. We believe that the high value for the Blue-fronted Amazon genome is potentially due to the application of multiple repeat finding strategies, as seen in other studies [S24]. Indeed, we observed a much higher proportion of repetitive genomic sequence with a combined approach (12.23%) than with RepeatMasker only (6.75%). Supporting this observation, a recent study that also used a combination of repeat-finding methodologies reported higher repetitive sequence content estimates than earlier analyses in chicken (13.28%) and zebra finch (12.83%) [S25], although estimates were still low for other avian species in the same work (Peregrine Falcon, 6.69%; Saker Falcon, 6.80%; turkey, 9.62%). The fact that avian genomes with the highest levels of sequence coverage, including Blue-fronted Amazon, present the highest estimates of repetitive content, suggests that high coverage sequencing may be required for more accurate estimates of repetitive genomic sequence. These values are still all lower than in mammals, where repetitive sequence elements account for a large proportion of the total genome sequence, with estimates of up to 45% in humans [S26].

UCNE ID	Average sequence deviation, parrots	Average sequence deviation, non-parrots	phylogenetic ANOVA	UCNE length (bp)
chr8_Ariane	10%	3%	9.99E-04	208
chr21_Gandalf	10%	3%	9.99E-03	200
ZC3H3_Roxane	7%	1%	9.99E-04	257
AUTS2_Ariel	7%	3%	1.20E-02	214
MIR4307_Noah	7%	4%	2.50E-02	224
ZNF608_Scheherazade	7%	4%	4.10E-02	299
BCL11A_Xavier	6%	1%	9.99E-04	201
chr5_Mateo	6%	2%	2.00E-03	208
SP8_Scarlett	6%	2%	7.99E-03	215
chr17_Bryan	6%	2%	1.50E-02	274
chr3_Eduardo	5%	2%	2.00E-03	294
chr15_Chen	5%	2%	3.00E-03	516
NPAS3_Jacob	5%	2%	4.00E-03	243
PROX1_Pablo	5%	1%	7.99E-03	208
ERBB4_Scheherazade	5%	2%	7.99E-03	247
SOX6_Julia	5%	2%	2.40E-02	250
chr2_Naomi	5%	2%	3.10E-02	206
ESRRG_Isolde	5%	2%	3.80E-02	213
EBF3_Isaac	5%	3%	4.60E-02	276
BCL11A_Zeus	5%	3%	4.95E-02	203

Table S5. Ultra-conserved noncoding elements (UCNEs) divergent in parrots. Related to STAR Methods.

Consensus chicken sequences for 4,351 UCNEs were obtained from a previous analysis [S27]. 20 of these were found to be divergent in parrots from the consensus chicken sequence by 5% or more, and significantly more divergent in parrots relative to other avian genomes (phylogenetic ANOVA, $\alpha < 0.05$).

Supplemental References

- S1. Tsolou, A., Nelson, G., Trachana, V., Chondrogianni, N., Saretzki, G., von Zglinicki, T., and Gonos, E.S. (2012). The 19S proteasome subunit Rpn7 stabilizes DNA damage foci upon genotoxic insult. *IUBMB Life* 64, 432-442.
- S2. Filippov, V., Filippova, M., and Duerksen-Hughes, P.J. (2007). The Early Response to DNA Damage Can Lead to Activation of Alternative Splicing Activity Resulting in CD44 Splice Pattern Changes. *Cancer Research* 67, 7621-7630.
- S3. Lei, K., Zhu, X., Xu, R., Shao, C., Xu, T., Zhuang, Y., and Han, M. (2012). Inner Nuclear Envelope Proteins SUN1 and SUN2 Play a Prominent Role in the DNA Damage Response. *Current Biology* 22, 1609-1615.
- S4. Elhassan, M.O., Christie, J., and Duxbury, M.S. (2012). Homo sapiens Systemic RNA Interference-defective-1 Transmembrane Family Member 1 (SIDT1) Protein Mediates Contact-dependent Small RNA Transfer and MicroRNA-21-driven Chemoresistance. *Journal of Biological Chemistry* 287, 5267-5277.
- S5. Xiong, D., Li, G., Li, K., Xu, Q., Pan, Z., Ding, F., Vedell, P., Liu, P., Cui, P., Hua, X., et al. (2012). Exome sequencing identifies MXRA5 as a novel cancer gene frequently mutated in non-small cell lung carcinoma from Chinese patients. *Carcinogenesis* 33, 1797-1805.
- S6. Prabhakar, S., Noonan, J.P., Pääbo, S., and Rubin, E.M. (2006). Accelerated Evolution of Conserved Noncoding Sequences in Humans. *Science* 314, 786-786.
- S7. Pollard, K.S., Salama, S.R., King, B., Kern, A.D., Dreszer, T., Katzman, S., Siepel, A., Pedersen, J.S., Bejerano, G., Baertsch, R., et al. (2006). Forces Shaping the Fastest Evolving Regions in the Human Genome. *PLoS Genet* 2, e168.
- S8. Jarvis, E.D., Mirarab, S., Aberer, A.J., Li, B., Houde, P., Li, C., Ho, S.Y.W., Faircloth, B.C., Nabholz, B., Howard, J.T., et al. (2014). Whole-genome analyses resolve early branches in the tree of life of modern birds. *Science* 346, 1320-1331.
- S9. Tacutu, R., Craig, T., Budovsky, A., Wuttke, D., Lehmann, G., Taranukha, D., Costa, J., Fraifeld, V.E., and de Magalhães, J.P. (2013). Human Ageing Genomic Resources: Integrated databases and tools for the biology and genetics of ageing. *Nucleic Acids Research* 41, D1027-D1033.
- S10. Prinzinger, R. (1993). Life span in birds and the ageing theory of absolute metabolic scope. *Comparative Biochemistry and Physiology Part A: Physiology* 105, 609-615.
- S11. Kim, N.W., Piatyszek, M.A., Prowse, K.R., Harley, C.B., West, M.D., Ho, P.L., Coviello, G.M., Wright, W.E., Weinrich, S.L., and Shay, J.W. (1994). Specific association of human telomerase activity with immortal cells and cancer. *Science* 266, 2011-2015.
- S12. Elowe, S. (2011). Bub1 and BubR1: at the Interface between Chromosome Attachment and the Spindle Checkpoint. *Molecular and Cellular Biology* 31, 3085-3093.
- S13. Wu, G., Zhou, L., Khidr, L., Guo, X.E., Kim, W., Lee, Y.M., Krasieva, T., and Chen, P.-L. (2008). A novel role of the chromokinesin Kif4A in DNA damage response. *Cell Cycle* 7, 2013-2020.
- S14. Loeb, K.R., Kostner, H., Firpo, E., Norwood, T., D. Tsuchiya, K., Clurman, B.E., and Roberts, J.M. (2005). A mouse model for cyclin E-dependent genetic instability and tumorigenesis. *Cancer Cell* 8, 35-47.
- S15. Hillier, L.W., Miller, W., Ewan Birney, Warren, W., Hardison, R.C., Ponting, C.P., Bork, P., Burt, D.W., Groenen, M.A.M., Delany, M.E., et al. (2004). Sequence and comparative analysis of the chicken genome provide unique perspectives on vertebrate evolution. *Nature* 432, 695-716.
- S16. Warren, W.C., Clayton, D.F., Ellegren, H., Arnold, A.P., Hillier, L.W., Kunstner, A., Searle, S., White, S., Vilella, A.J., Fairley, S., et al. (2010). The genome of a songbird. *Nature* 464, 757-762.
- S17. Koren, S., Schatz, M.C., Walenz, B.P., Martin, J., Howard, J.T., Ganapathy, G., Wang, Z., Rasko, D.A., McCombie, W.R., Jarvis, E.D., et al. (2012). Hybrid error correction and *de novo* assembly of single-molecule sequencing reads. *Nat Biotech* 30, 693-700.
- S18. Ganapathy, G., Howard, J., Ward, J., Li, J., Li, B., Li, Y., Xiong, Y., Zhang, Y., Zhou, S., Schwartz, D., et al. (2014). High-coverage sequencing and annotated assemblies of the budgerigar genome. *GigaScience* 3, 11.
- S19. Oleksyk, T., Pombert, J.-F., Siu, D., Mazo-Vargas, A., Ramos, B., Guiblet, W., Afanador, Y., Ruiz-Rodriguez, C., Nickerson, M., Logue, D., et al. (2012). A locally funded Puerto Rican parrot (*Amazona vittata*) genome sequencing project increases avian data and advances young researcher education. *GigaScience* 1, 14.

- S20. Seabury, C.M., Dowd, S.E., Seabury, P.M., Raudsepp, T., Brightsmith, D.J., Liboriussen, P., Halley, Y., Fisher, C.A., Owens, E., Viswanathan, G., et al. (2013). A Multi-Platform Draft *de novo* Genome Assembly and Comparative Analysis for the Scarlet Macaw (*Ara macao*). PLoS ONE 8, e62415.
- S21. Zhang, G., Li, C., Li, Q., Li, B., Larkin, D.M., Lee, C., Storz, J.F., Antunes, A., Greenwold, M.J., Meredith, R.W., et al. (2014). Comparative genomics reveals insights into avian genome evolution and adaptation. Science 346, 1311-1320.
- S22. van der Zwan, H., van der Westhuizen, F., Visser, C., and van der Sluis, R. (2017). Draft De Novo Genome Sequence of *Agapornis roseicollis* for Application in Avian Breeding. Animal Biotechnology, 1-6.
- S23. Doyle, J.M., Katzner, T.E., Bloom, P.H., Ji, Y., Wijayawardena, B.K., and DeWoody, J.A. (2014). The Genome Sequence of a Widespread Apex Predator, the Golden Eagle (*Aquila chrysaetos*). PLoS ONE 9, e95599.
- S24. Lerat, E. (2010). Identifying repeats and transposable elements in sequenced genomes: how to find your way through the dense forest of programs. Heredity 104, 520-533.
- S25. Zhan, X., Pan, S., Wang, J., Dixon, A., He, J., Muller, M.G., Ni, P., Hu, L., Liu, Y., Hou, H., et al. (2013). Peregrine and saker falcon genome sequences provide insights into evolution of a predatory lifestyle. Nat Genet 45, 563-566.
- S26. International Human Genome Sequencing Consortium (2001). Initial sequencing and analysis of the human genome. Nature 409, 860-921.
- S27. Dimitrieva, S., and Bucher, P. (2013). UCNEbase—a database of ultraconserved non-coding elements and genomic regulatory blocks. Nucleic Acids Research 41, D101-D109.